

# Discovery and SAR of Novel 2,3-Dihydroimidazo[1,2-c]-quinazoline PI3K Inhibitors: Identification of Copanlisib (BAY 80-6946)

William J. Scott,<sup>\*,[a]</sup> Martin F. Hentemann,<sup>[c]</sup> R. Bruce Rowley,<sup>[c]</sup> Cathy O. Bull,<sup>[c]</sup> Susan Jenkins,<sup>[c]</sup> Ann M. Bullion,<sup>[c]</sup> Jeffrey Johnson,<sup>[c]</sup> Anikó Redman,<sup>[c]</sup> Arthur H. Robbins,<sup>[c]</sup> William Esler,<sup>[c]</sup> R. Paul Fracasso,<sup>[c]</sup> Timothy Garrison,<sup>[c]</sup> Mark Hamilton,<sup>[c]</sup> Martin Michels,<sup>[d]</sup> Jill E. Wood,<sup>[c]</sup> Dean P. Wilkie,<sup>[c]</sup> Hong Xiao,<sup>[c]</sup> Joan Levy,<sup>[c]</sup> Enrico Stasik,<sup>[e]</sup> Ningshu Liu,<sup>[e]</sup> Martina Schaefer,<sup>[f]</sup> Michael Brands,<sup>[b]</sup> and Julien Lefranc<sup>\*,[b]</sup>

*Dedicated to the memory of Bruce Rowley, a friend and colleague.*

The phosphoinositide 3-kinase (PI3K) pathway is aberrantly activated in many disease states, including tumor cells, either by growth factor receptor tyrosine kinases or by the genetic mutation and amplification of key pathway components. A variety of PI3K isoforms play differential roles in cancers. As such, the development of PI3K inhibitors from novel compound classes should lead to differential pharmacological and pharmacokinetic profiles and allow exploration in various indications, combinations, and dosing regimens. A screening effort aimed at

the identification of PI3K $\gamma$  inhibitors for the treatment of inflammatory diseases led to the discovery of the novel 2,3-dihydroimidazo[1,2-c]quinazoline class of PI3K inhibitors. A subsequent lead optimization program targeting cancer therapy focused on inhibition of PI3K $\alpha$  and PI3K $\beta$ . Herein, initial structure–activity relationship findings for this class and the optimization that led to the identification of copanlisib (BAY 80-6946) as a clinical candidate for the treatment of solid and hematological tumors are described.

## Introduction

The phosphoinositide 3-kinase (PI3K) family of lipid kinases generates 3'-phosphoinositides that bind to and activate a variety of cellular targets, initiating a wide range of signal transduction cascades.<sup>[1–3]</sup> These cascades ultimately induce changes in a range of cellular processes including proliferation, survival, differentiation, migration, vesicle trafficking, and chemotaxis.

Class I PI3Ks transmit signals downstream of transmembrane receptors, signaling from receptor tyrosine kinases via p110 $\alpha$ , p110 $\beta$  and p110 $\delta$  isoforms, and from G-protein-coupled receptors via p110 $\beta$  and p110 $\gamma$  isoforms. Class I PI3Ks are divided into two distinct subclasses based on differences in protein subunit composition. The class I $\alpha$  PI3Ks are comprised of a catalytic p110 subunit (p110 $\alpha$ , p110 $\beta$  or p110 $\delta$ ) heterodimerized with a member of the p85 regulatory subunit family. The class I $\alpha$  PI3K isoforms associate with activated receptor tyrosine kinases (RTKs) (including PDGFR, EGFR, VEGFR, IGF1-R, c-KIT, CSF-R and Met), or with tyrosine phosphorylated adapter proteins, via their p85 regulatory subunits, resulting in stimulation of the lipid kinase activity.

In contrast, the class I $\beta$  PI3Ks are comprised of a catalytic p110 subunit (p110 $\gamma$ ) heterodimerized with a distinct p101 regulatory subunit.<sup>[4,5]</sup> Activation of class I PI3K-mediated signaling has been directly linked to cancer. Somatic mutations or amplification of the gene encoding human p110 $\alpha$  (PIK3CA) is known to be causative in many cancers.<sup>[5–8]</sup> Overexpression or mutational activation of RTKs leading to increased PI3K signaling occurs in multiple tumor types.<sup>[5,9]</sup> Loss of function or inactivation of the tumor suppressor PTEN (phosphatase and tensin homologue) also leads to increased PI3K signaling and tumor growth.<sup>[10–12]</sup> This appears to be mediated via the p110 $\beta$  isoform.<sup>[13–15]</sup> In addition, aberrant activation of class I PI3Ks has been associated with both intrinsic and acquired resistance to targeted therapeutic agents, such as lapatinib or vemurafenib.

[a] Dr. W. J. Scott

Global Development, Global Program Management, Bayer HealthCare Pharmaceuticals Inc., Whippany, NJ 07981 (USA)  
E-mail: william.scott@bayer.com

[b] Prof. Dr. M. Brands, Dr. J. Lefranc

Global Drug Discovery, Medicinal Chemistry Berlin, Bayer Pharma AG, 13353 Berlin (Germany)  
E-mail: julien.lefranc@bayer.com

[c] Dr. M. F. Hentemann, Dr. R. B. Rowley, C. O. Bull, Dr. S. Jenkins, A. M. Bullion,

J. Johnson, A. Redman, Dr. A. H. Robbins, W. Esler, Dr. R. P. Fracasso, T. Garrison, Dr. M. Hamilton, Dr. J. E. Wood, D. P. Wilkie, H. Xiao, Dr. J. Levy  
Former Bayer Research Center, West Haven, CT 16516 (USA)

[d] Dr. M. Michels

Global Drug Discovery, Project Management Drug Discovery, Bayer Pharma AG, 13353 Berlin (Germany)

[e] E. Stasik, Dr. N. Liu

Global Drug Discovery, TRG Oncology, Bayer Pharma AG, 13353 Berlin (Germany)

[f] Dr. M. Schaefer

Global Drug Discovery, Structural Biology, Bayer Pharma AG, 13353 Berlin (Germany)

Supporting information for this article can be found under <http://dx.doi.org/10.1002/cmdc.201600148>.

nib,<sup>[16–18]</sup> as well as resistance to traditional cytotoxic chemotherapy and radiation therapy.<sup>[19–21]</sup>

A number of PI3K/mTOR, pan-PI3K and selective PI3K inhibitors have entered early clinical development.<sup>[3,22–25]</sup> Idelalisib (Figure 1), a PI3K $\delta$ -selective inhibitor, has recently been approved for use in the treatment of two subtypes of indolent non-Hodgkin's lymphoma.<sup>[26]</sup> In contrast, the clinical benefit of PI3K inhibition in solid tumors has yet to be clearly demonstrated. This is largely due to the following factors: 1) feedback activation of physiologic signaling in tumors,<sup>[27–29]</sup> 2) selectivity to PI3K and disease relevant PI3K isoforms, 3) both on-target and off-target toxicity. These factors limited pathway inhibition and efficacy. Accordingly, there remains a need for the development of novel PI3K inhibitors with differing pharmacologic and pharmacokinetic profiles.

Guided by X-ray crystallographic structures of first-generation PI3K inhibitors bound to PI3K $\gamma$ , it has been shown that in-

teraction with the protein hinge region is obligatory, and activity can be enhanced via affinity pocket interactions.<sup>[30–32]</sup> This led to the development of two major classes of PI3K inhibitors (Figure 1). There is a family of morpholine-based inhibitors, typified by pictilisib, buparlisib and apitolisib, having hinge binding with the relatively weak hydrogen-bond-accepting morpholine oxygen, and having strong affinity pocket interactions, typically involving both a hydrogen-bond acceptor and a hydrogen-bond donor.<sup>[33]</sup> In contrast, PI3K $\delta$ -selective inhibitors, such as idelalisib, PIK-39 and AMG-319, possess strong hinge interactions via a purine moiety combined with induction of a selectivity pocket.<sup>[34–36]</sup> A novel approach might involve discovery of a compound class that allows both strong binding at the hinge and strong affinity pocket interactions. Herein, we describe the optimization of the 2,3-dihydroimidazo[1,2-*c*]quinazoline class of PI3K inhibitors which strongly bind at both critical sites, leading to the discovery of copanlisib.

## Results and Discussion

### Structure–activity relationships of 2,3-dihydroimidazo[1,2-*c*]quinazoline PI3K inhibitors

Initial interest in PI3K inhibitors at Bayer centered around the development of PI3K $\gamma$  inhibitors as anti-inflammatory agents with potential as anti-asthmatic agents.<sup>[37]</sup> High-throughput screening for PI3K $\gamma$ -active leads led to the discovery of the novel lead 2,3-dihydroimidazo[1,2-*c*]quinazoline **1** (p110 $\gamma$  IC<sub>50</sub> = 810 nM, p110 $\beta$  IC<sub>50</sub> = 4000 nM) (Figure 2). During lead optimization efforts, it was established that the enol moiety of structure **1** could be replaced with an amide moiety to minimize potential for untoward reactivity. In addition, the phenyl substituent was replaced with a 3-pyridyl moiety, leading to analogue **2**. In addition, it was found that A-ring substitution, such as in compound **3**, could affect isoform activity ratios. With this information in hand, a program to optimize the p110 $\beta$  and p110 $\alpha$  activity of the 2,3-dihydroimidazo[1,2-*c*]quinazoline lead for potential use in cancer therapies was undertaken.

Docking of 2,3-dihydroimidazo[1,2-*c*]quinazolines with the published structure for p110 $\gamma$ ,<sup>[31]</sup> and making the assumption that the inhibitors are bound to the ATP binding site, led to the hypothesis that the dihydroimidazole N1 nitrogen binds at the protein hinge, while the C-ring sp<sup>3</sup> carbons fill a nearby hydrophobic pocket. Modeling also suggested that the C5 heter-

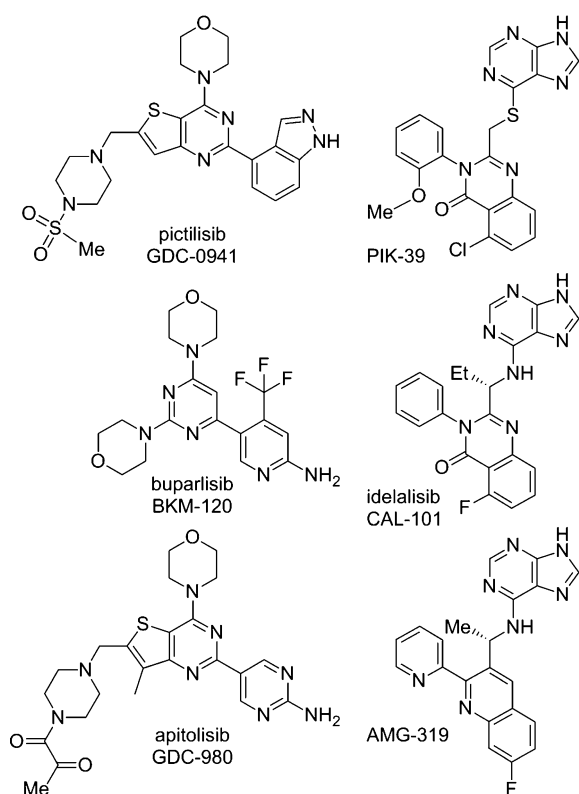


Figure 1. PI3K inhibitors.

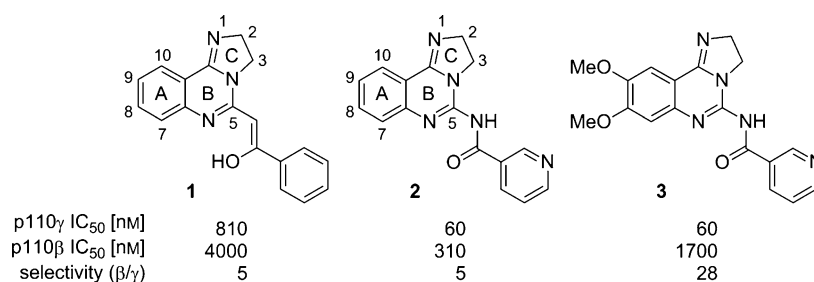
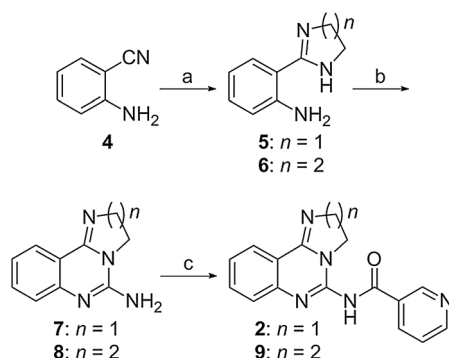


Figure 2. Optimization of the initial lead.

ocyclic amide moiety occupies a pocket not used by ATP, and offers potential hydrogen-bonding opportunities. In addition, C7 was predicted to point toward the ATP sugar pocket and C8 toward a channel leading to solvent. Thus, initial synthetic efforts were directed toward confirmation of the binding hypothesis, as well as toward inhibitor optimization. The binding model was substantiated after the conclusion of the optimization program, via an X-ray structure of copanlisib (**39i**) bound to p110 $\gamma$  (see below).

### Synthetic strategy

C-ring SAR was explored during early studies directed toward development of PI3K $\gamma$  inhibitors by variation of the diamine used for imidazoline synthesis.<sup>[37]</sup> Unsubstituted 2,3-dihydroimidazo[1,2-c]quinazoline, **2**, was synthesized starting from 2-cyanoaniline (**4**) by treatment with ethylenediamine in the presence of phosphorus pentasulfide, which afforded aniline **5** (Scheme 1). Cyclization with cyanogen bromide led to tricyclic amine **7**, which was acylated to afford amide **2**. The corresponding ring-expanded 3,4-dihydro-2H-pyrimido[1,2-c]quinazoline **9** was synthesized in an analogous manner using 1,3-propylenediamine.

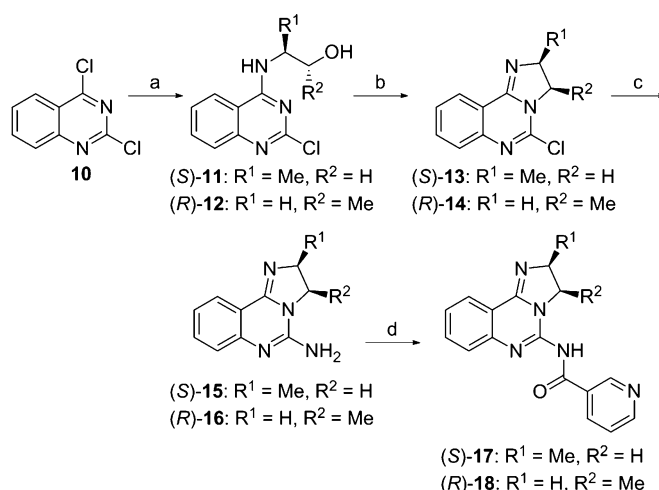


**Scheme 1.** Synthesis of C-ring analogues **2** and **9**.<sup>[37]</sup> Reagents and conditions: a)  $\text{H}_2\text{N}(\text{CH}_2)_{n+1}\text{NH}_2$ ,  $\text{P}_2\text{S}_5$ , 0 to 100 °C; b)  $\text{BrCN}$ , MeOH; c) nicotinic acid, PyBOP, Hünig's base, DMF.

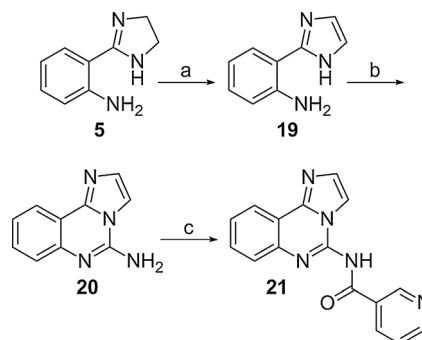
To examine the effect of substitution on the C-ring, dichloroquinazoline **10** was treated with the appropriate chiral amino-propanol, and the resulting alcohols **11** and **12** were cyclized to afford 5-chloro-2,3-dihydroimidazoquinazolines **13** and **14** (Scheme 2). The quinazolines were treated with ammonia, followed by nicotinic acid to afford amides **17** and **18**.

The effect of the C-ring oxidation state on efficacy was examined using imidazo[1,2-c]quinazoline **21**. Thus, oxidation ( $\text{MnO}_2$ ) of aminodihydroimidazole **5** to aminoimidazole **19** was followed by cyclization with cyanogen bromide to give **20** and then by acylation with nicotinic acid to afford amide **21** (Scheme 3).

To study variation at the C5, C7, and C8 positions, a more general approach involving preparation of key intermediate **29** was envisioned (Scheme 4). The synthesis began with treatment of vanillin acetate (**22**) with fuming nitric acid to readily



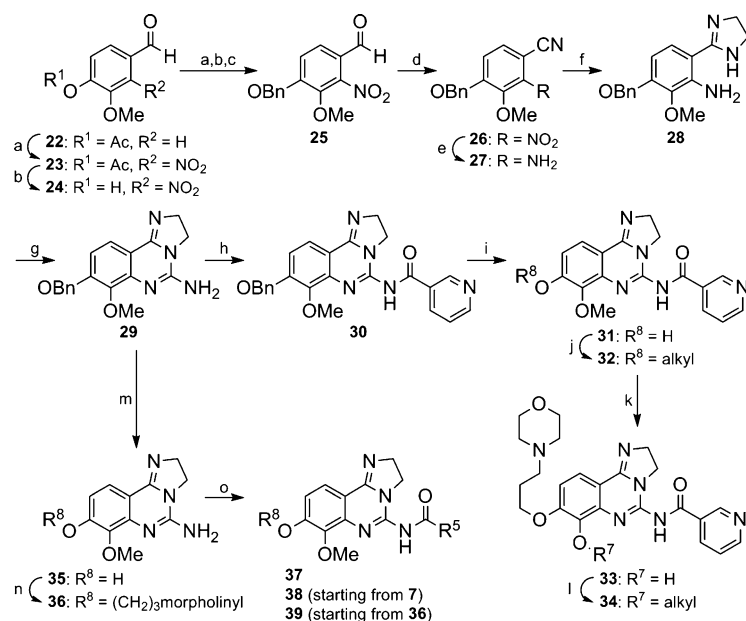
**Scheme 2.** Synthesis of C-ring analogues **17** and **18**.<sup>[37]</sup> Reagents and conditions: a)  $\text{H}_2\text{NCH(R}^1\text{)CH(R}^2\text{)OH}$ , TEA, THF, quant.; b)  $\text{POCl}_3$  (crude product used in the next step); c) aq.  $\text{NH}_3$ , 150 °C, 12% (**15**), 17% (**16**); d) nicotinic acid, PyBOP, Hünig's base, DMF, 80 °C, 28% (**17**), 35% (**18**).



**Scheme 3.** Synthesis of C-ring analogue **21**.<sup>[37]</sup> Reagents and conditions: a)  $\text{MnO}_2$ , DMPU, 150 °C, 61%; b)  $\text{BrCN}$ , MeOH, 61%; c) nicotinic acid, PyBOP, Hünig's base, DMF, 80 °C, 20%.

afford known aldehyde **23**.<sup>[38,39]</sup> Conversion into benzyl ether **25** followed by ammonium hydroxide/iodine oxidation gave nitrile **26**. Reduction provided aniline **27**, and treatment with ethylenediamine allowed formation of the C-ring. Imidazoline **28** was then cyclized using cyanogen bromide to give tricyclic amine **29**, which was acylated using classical peptide-coupling conditions to provide amide **30**. Treatment of amide **30** with trifluoroacetic acid afforded deprotected phenol **31**, which could then be alkylated at C8 giving access to the aryl ethers, **32**.

The C7 methyl ethers of 8-alkoxy-7-methoxy analogues proved labile to sulfide-based hydrolysis, likely due to the more hindered methoxy being forced outside of the dihydroimidazoquinazoline plane.<sup>[40,41]</sup> Alkylation of the phenol **33** resulting from hydrolysis of analogue **32g** [ $\text{R}^8 = 3\text{-(morpholin-4-yl)propyl}$ ] led to the desired C7 aryl ethers **34**. Alternatively, debenzoylation of quinazoline **29** at C8 could be achieved using trifluoroacetic acid. The resulting phenol, **35**, was readily converted into amine **36**, which upon acylation to **37** could be used to investigate the amide SAR.



**Scheme 4.** General synthetic approach to analogues for SAR studies. *Reagents and conditions:* a) fuming  $\text{HNO}_3$ ,  $< 10^\circ\text{C}$ , 41%; b)  $\text{K}_2\text{CO}_3$ , MeOH, 88%; c)  $\text{BnBr}$ ,  $\text{K}_2\text{CO}_3$ , DMF, 97%; d)  $\text{NH}_4\text{OH}$  (28%),  $\text{I}_2$ , THF, 95%; e)  $\text{Fe}$ ,  $\text{AcOH}$ ,  $\text{H}_2\text{O}$ ,  $5^\circ\text{C}$  to RT, 88%; f)  $\text{H}_2\text{N}(\text{CH}_2)_2\text{NH}_2$ ,  $\text{S}_8$ ,  $100^\circ\text{C}$ , 86%; g)  $\text{BrCN}$ , TEA,  $\text{CH}_2\text{Cl}_2$ ,  $0^\circ\text{C}$  to RT, quant.; h) nicotinic acid, PyBOP, Hünig's base, DMF, 98%; i) TFA,  $60^\circ\text{C}$ , 66%; j)  $\text{R}^8\text{X}$ , base, DMF; k)  $\text{Na}_2\text{S}$ , NMP,  $160^\circ\text{C}$ , 51% [ $\text{R}^8 = 3$ -(morpholin-4-yl)propyl, **32g**]; l)  $\text{R}^7\text{X}$ , base, DMF; m) TFA,  $60^\circ\text{C}$ , crude starting material was used; n) 3-(morpholin-4-yl)propyl chloride,  $\text{Cs}_2\text{CO}_3$ , DMF,  $70^\circ\text{C}$ , 44%; o)  $\text{R}^5\text{CO}_2\text{H}$ , PyBOP, Hünig's base, DMF.

### C-ring SAR

Initially, C-ring SAR was probed (Table 1). The binding hypothesis suggested that the pocket filled by ring C left little room for modification. Consistent with this, expansion to the six-membered C-ring led to the completely inactive tetrahydropyrimidine, **9**. Similarly, activity was lost when a methyl group was introduced at either C2 or C3 (compounds **17** and **18**). Oxidation of the five-membered ring to the corresponding imidazole **21** resulted in decreased activity, by a factor of five relative to dihydroimidazole **2**. Based on these initial results, there were no further attempts to optimize SAR at the C-ring. The inability to accommodate C-ring substitution was later validated with an X-ray structure of copanlisib (**39i**) bound to p110 $\gamma$  (see below).

### A-ring C8 SAR

The binding hypothesis suggested that substituents at C8 would fit into a channel pointing toward solvent. To probe this, modifications at the C8 position were investigated (Table 2). Benzyl ether **30** and phenol **31** were highly potent against p110 $\alpha$ ; however, they showed decreased activity against p110 $\beta$  relative to methoxy analogue **32a**. Exchanging the methyl ether for the ethyl ether (**32b**) had little influence on the potency but the bulkier isobutyl ether **32c** was seven-fold less potent against p110 $\beta$ .

Consistent with the binding model, addition of a polar moiety attached via an alkoxy linker was tolerated. Thus, aminopropoxy analogue **32d** and the corresponding dimethyla-

mine, **32e**, showed potency against p110 $\alpha$  similar to that of methoxy analogue **32a**; however, they were slightly more potent against p110 $\beta$ . Expanding the bulk around the amine, such as with piperidine **32f** or morpholine **32g**, slightly improved p110 $\alpha$  potency without modifying the activity against p110 $\beta$ . The length of the linker between the morpholine moiety and the core was also investigated. Thus, compound **32h**, bearing a two-carbon linker, showed improved activity however it appeared to be chemically unstable, while analogue **32i**, bearing a four-carbon linker, showed a drop in potency. In summary, variation of the alkoxy moiety at C8 had little effect on p110 $\alpha$  potency. In contrast, activity against p110 $\beta$  proved somewhat more sensitive.

Inclusion of an amine base tethered to the core via an alkyl ether appeared optimal. Compounds with strong nitrogen bases at C8, such as amine **32d**, dimethylamine **32e** or piperidine **32f**, led to high clearance in PK studies (data not shown), and were not further pursued.

### A-ring C7 SAR

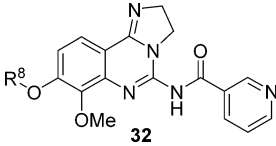
The binding hypothesis suggested that modifications at C7 might allow probing of the ATP sugar pocket. Variation of the C7 methoxy group of morpholine derivative **32g** was initiated by replacement with a propoxy moiety (**34a**). An increase in potency against p110 $\beta$  was observed in the biochemical assay (Table 3); however, this effect did not translate to the cellular assays (data not

**Table 1.** C-ring SAR.

Compd	C-ring analogue	IC <sub>50</sub> [nM] <sup>[a]</sup>	
		p110 $\alpha$	p110 $\beta$
<b>2</b>		n.d.	192
<b>9</b>		n.d.	> 10 000
<b>17</b>		n.d.	> 10 000
<b>18</b>		> 1000	> 10 000
<b>21</b>		n.d.	1040

[a] n.d. = not determined.

Table 2. A-ring C8 SAR.



Compd	R <sup>8</sup> -O-	p110α	IC <sub>50</sub> [nM] <sup>[a]</sup> p110β
30		6.1	1510
31		8.7	210
32 a		4.5	30.7
32 b		3.6	76.1
32 c		8.0	226
32 d		4.7	22.3
32 e		3.6	18.0
32 f		2.9	18.3
32 g		1.8	20.8
32 h		0.9	11.2
32 i		n.d.	88.1

[a] n.d. = not determined.

shown). Neither allyl ether **34 b** nor isobutyl ether **34 c** offered any benefit over methyl ether **32 g**. In contrast, introduction of a cyclohexyl group (**34 d**) resulted in a significant decrease in activity against p110β. This could be recovered by addition of distal polarity, as in tetrahydropyran **34 e** or pyridine **34 f**. Because no significant improvement was achieved by modifying the substituents at C7, the initial methoxy moiety was chosen for additional studies in order to minimize molecular weight.

### B-ring C5 amide SAR

The strongest interactions predicted by the binding hypothesis involve the dihydroimidazole binding at the hinge, and interactions within the C5 heterocyclic amide pocket. Thus, optimization at C5 offered a high potential for improvements in activity, and a series of amide modification was undertaken multiple times during the program.

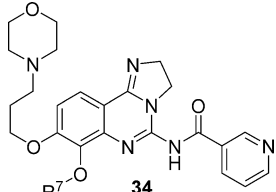
### Amides of A-ring-unsubstituted 5-amino-2,3-dihydroimidazo[1,2-c]quinazoline

An initial understanding of C5 amide SAR was developed using the A-ring-unsubstituted 2,3-dihydroimidazo[1,2-c]quinazoline system (Table 4).<sup>[31]</sup> Alkyl amides, such as acetamide **38 a** and cyclohexyl analogue **38 b**, were significantly less active than pyridine **2**. The same was observed for aryl amides, for example phenyl analogue **38 c** and thiazole **38 d**. This decreased activity may be due to the inability of these amides to act as hydrogen-bond acceptors. Inclusion of a hydrogen-bond acceptor in the 3'-position, such as in thiazole **38 e**, led to an activity equivalent to that of pyridine **2**, even in the presence of steric hindrance. Further addition of a hydrogen-bond donor, for example as in aminopyridine **38 f** or imidazopyridine **38 g**, resulted in a significant improvement in activity.

### Amides of 5-amino-7-methoxy-8-[3-(morpholin-4-yl)propoxy]-2,3-dihydroimidazo[1,2-c]quinazoline

C5 Amide SAR for compounds substituted at C8 with an aminoalkoxy group revealed similar trends to those observed for the C8-unsubstituted analogues (Table 5 vs. Table 4). Thus, the absence of a hydrogen-bond donor, such as in compound **39 a**, resulted in decreased activity against p110β, while thiazole **39 b** (a direct analogue of **38 e**) proved slightly more potent than **32 g** (Table 5). Moving the pyridine nitrogen from position 3' to 4' (**32 g** vs. **39 c**) led to reduced activity against p110β by a factor of three. Addition of a hydrogen-bond donor, such as an amino group on the pyridine ring as in analogues **39 d** and **39 e**, resulted in a slight increase in potency. However, dimethylation of the aminopyridine (**39 f**) led to a decrease in activity. Introduction of a second nitrogen in the ring, such as in pyrazine **39 g** and pyrimidine **39 h**, led to a significant drop in activity. Surprisingly, the activity could be recovered by introduction of a free amino group in the 4'-position of the pyrimidine (**39 i** and **39 j**); in the case of **39 j**, an additional methyl substituent was tolerated. Thus, activity was opti-

Table 3. A-ring C7 SAR.

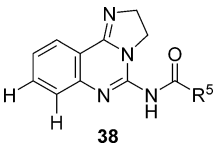
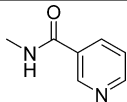
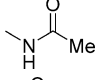
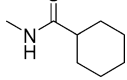
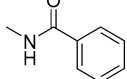
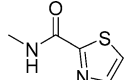
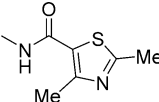
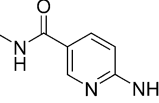
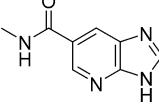


Compd	R <sup>7</sup> -O-	p110α	IC <sub>50</sub> [nM] <sup>[a]</sup> p110β
32 g		1.8	20.8
33		n.d.	55.6
34 a		n.d.	7.8
34 b		n.d.	22.6
34 c		10.2	29.1
34 d		n.d.	88.5
34 e		2.1	18.2
34 f		n.d.	19.3

[a] n.d. = not determined.



**Table 4.** SAR of amides of A-ring-unsubstituted 5-amino-2,3-dihydroimidazo[1,2-c]quinazoline.

			
Compd	$-\text{NH}-\text{C}(=\text{O})-\text{R}^5$	$\text{IC}_{50}$ [nM] <sup>[a]</sup> p110 $\alpha$	p110 $\beta$
2		n.d.	192
38 a		n.d.	1650
38 b		n.d.	> 10000
38 c		n.d.	71 260
38 d		n.d.	532
38 e		n.d.	176
38 f		12.0	49.3
38 g		n.d.	31.1

[a] n.d. = not determined.

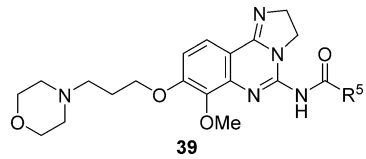
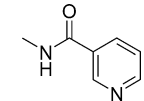
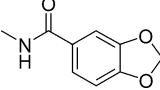
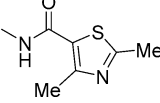
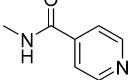
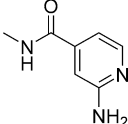
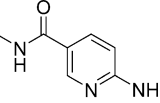
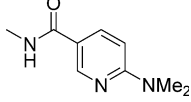
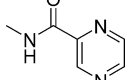
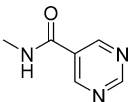
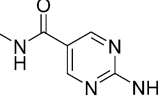
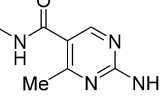
mized by the use of both a hydrogen-bond acceptor and a hydrogen-bond donor.

### Cellular screening

Selected compounds were tested in mechanistic and functional cellular assays, allowing differentiation of suitable candidates (Table 6). Cellular mechanistic activity of compounds was probed by investigating inhibition of AKT phosphorylation by PI3K.<sup>[42]</sup> KPL4, a breast cancer cell line that carries a *PIK3CA*-activating mutation, was selected for profiling of anti-proliferative effects.<sup>[42]</sup>

Relative activity in cellular assays generally paralleled that observed in the biochemical assays. Thus, C7-extended analogue **34 d** proved approximately equivalent to methyl ether **32 a**, while 4'-aminopyridine **39 e** was significantly more active. Surprisingly, 3'-aminopyridine **39 d** displayed significantly less

**Table 5.** SAR of amides of 5-amino-7-methoxy-8-[3-(morpholin-4-yl)propoxy]-2,3-dihydroimidazo[1,2-c]quinazoline.

			
Compd	$-\text{NH}-\text{C}(=\text{O})-\text{R}^5$	$\text{IC}_{50}$ [nM] <sup>[a]</sup> p110 $\alpha$	p110 $\beta$
32 g		1.8	20.8
39 a		20.9	668
39 b		1.6	7.8
39 c		n.d.	63.7
39 d		6.2	16.6
39 e		0.6	7.9
39 f		2.9	58.7
39 g		n.d.	351
39 h		132	286
39 i (copanlisib, BAY 80-6946)		0.5	3.7
39 j		0.4	1.0

[a] n.d. = not determined.

activity than expected in the mechanistic assay. Consistent with the biochemical data, aminopyrimidine **39 i** and 2'-amino-4'-methylpyrimidine **39 j** proved optimal in cellular assays.

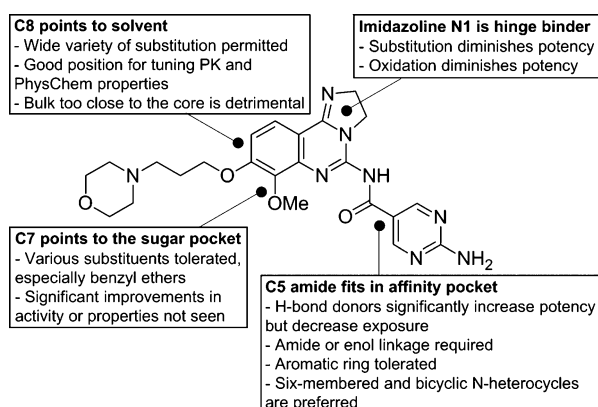
**Table 6.** Mechanistic and functional cellular activity of selected compounds.

	32a <sup>[a]</sup>	34d <sup>[a]</sup>	39b	39d <sup>[a]</sup>	39e <sup>[a]</sup>	39i	39j
p110 $\alpha$ IC <sub>50</sub> [nM]	4.5	n.d.	1.6	6.2	0.6	0.5	0.4
p110 $\beta$ IC <sub>50</sub> [nM]	30.7	88.5	7.8	16.6	7.9	3.7	1.0
IGF-1-stimulated A549 pAKT(S473) IC <sub>50</sub> [nM]	30	55	60	170	11	3.4	0.6
KPL4 proliferation EC <sub>50</sub> [nM]	n.d.	n.d.	86	n.d.	n.d.	3.7	2.3

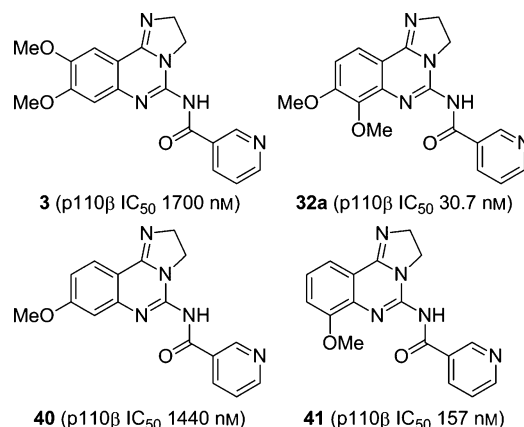
[a] n.d. = not determined.

### SAR summary

In summary (see Figure 3), modification of the imidazoline C-ring, either by substitution, oxidation or ring expansion, resulted in a loss of activity, supporting the hypothesis that the N1 nitrogen is involved in hinge binding. The aromatic C5 amide proved to be the key driver of potency. The amide should preferably have a five- or six-membered monocyclic, or bicyclic, nitrogen-containing heterocycle. Inclusion of a hydrogen-bond donor significantly increased potency, but at the expense of decreased water solubility and oral bioavailability. The optimal amide contained an aminopyrimidine moiety.

**Figure 3.** SAR summary.

Substitution at C7 affords SAR consistent with occupation of a pocket amenable to polar interactions. Unfortunately, while tolerated, substitution did not lead to increased potency or beneficial properties. Thus, the C7 methoxy moiety was considered optimal. The SAR indicated that inclusion of polar groups at C8 allowed the tuning of water solubility and PK properties. Aminoalkoxy substituents were optimal, and balancing of activity with PK properties led to the selection of a 3-morpholinylpropoxy moiety at C8 (Figure 3). Thus, overall optimization led to the selection of analogue **39i**, copanlisib (BAY 80-6946), for further development. In addition, relative to 7,8-dimethoxy compound **32a**, 8,9-dimethoxy analogue **3** was significantly less active (Figure 4). Removal of either the C7 methoxy moiety (analogue **40**) or the C8 methoxy moiety (analogue **41**) from **32a** led to decreased activity. This led to the conclusion that substitution at both C7 and C8 was optimal.

**Figure 4.** Influence of A-ring C7/C8/C9 substitution.

### Binding mode

After the conclusion of the optimization program, an X-ray structure of copanlisib (**39i**) bound to p110 $\gamma$  was determined. The structure is in general agreement with that previously reported for dimethoxy analogue **32a** bound to p110 $\gamma$ .<sup>[32]</sup> The imidazoline N1 nitrogen forms a critical hydrogen bond to Val882 in the adenine pocket (Figure 5). The majority of known PI3K $\alpha$  inhibitors use a morpholine oxygen for this interaction.<sup>[32,33]</sup>

The C5 aminopyrimidine group fills the affinity pocket, forming hydrogen bonds with Asp836 and Asp841 through the amino group, and with Lys833 through a pyrimidine nitrogen. In addition, Asp964 appears to contribute a pi-stacking interaction. Finally, the morpholine group of copanlisib lies over Trp812, apparently adding a hydrophilic shield to the hydrophobic heterocycle. The binding hypothesis, as validated by the X-ray structure, provides a structural rationale for and validation of the conclusions generated from the SAR studies.

### Pharmacology

The pharmacology of copanlisib (**39i**) has been described in detail elsewhere,<sup>[42]</sup> the results are summarized in Table 7. Copanlisib is a potent class I PI3K inhibitor with preferential activity against p110 $\alpha$  and p110 $\delta$  as compared with p110 $\beta$  and p110 $\gamma$ . Copanlisib has potent cellular mechanistic activity, inhibiting both IGF-1-stimulated AKT phosphorylation in A549 cells, and basal AKT phosphorylation in KPL4 cells. This translated to the potent inhibition of proliferation in many cell lines,<sup>[42]</sup> as exemplified by KPL4.

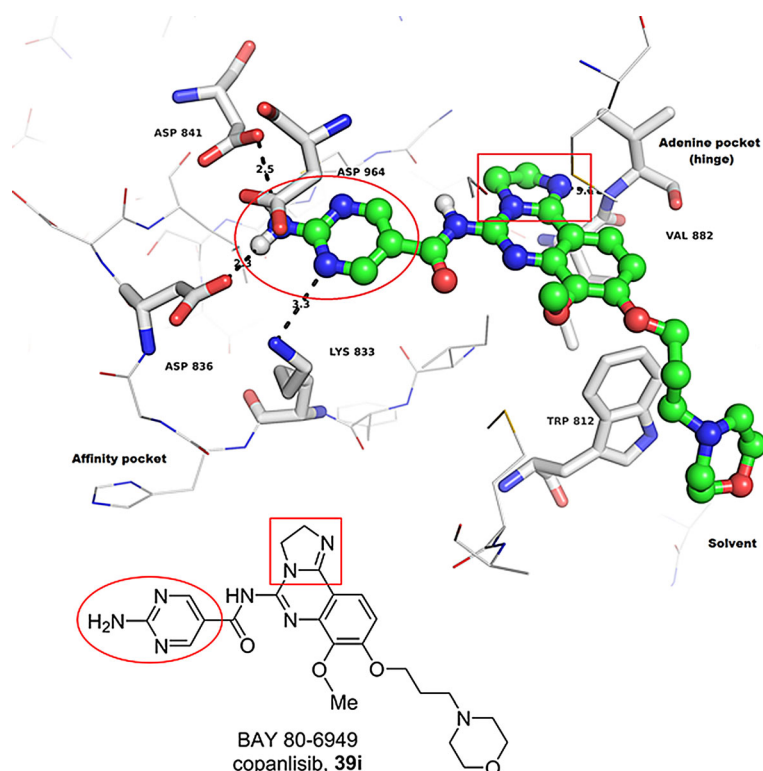


Figure 5. X-ray crystal structure of copanlisib bound to PI3K $\gamma$ .

Table 7. Pharmacology profile of copanlisib (**39i**).

Profile	Value
<b>Biochemical profile</b>	
p110 $\alpha$ IC <sub>50</sub> [nM]	0.5
p110 $\beta$ IC <sub>50</sub> [nM]	3.7
p110 $\gamma$ IC <sub>50</sub> [nM]	6.4
p110 $\delta$ IC <sub>50</sub> [nM]	0.7
mTOR kinase IC <sub>50</sub> [nM]	45
Panel of 220 kinases (10 $\mu$ M)	< 50% inhibition
<b>Cellular mechanistic profile (pAKT-S473)</b>	
PI3K $\alpha$ (KPL4) IC <sub>50</sub> [nM]	0.4
PI3K $\beta$ (LPA-stimulated PC3) IC <sub>50</sub> [nM]	10
PI3K $\gamma$ (C5a-stimulated Raw 264.7) IC <sub>50</sub> [nM]	94
PI3K $\delta$ (IgM-stimulated Raji) IC <sub>50</sub> [nM]	7.4
mTOR (p-4E-BP1-S65 in ELT3) IC <sub>50</sub> [nM]	> 500
<b>In vitro antiproliferative activity IC<sub>50</sub> [nM]</b>	
KPL4 (PIK3CA <sup>mut</sup> ) IC <sub>50</sub> [nM]	3.7
ZR-75-1 (PTEN <sup>loss</sup> ) IC <sub>50</sub> [nM]	24
TMD-8 (CD79 <sup>mut</sup> ) IC <sub>50</sub> [nM]	2.3
<b>In vivo activity [% TGI]<sup>[a]</sup></b>	
KPL4 (14 mg kg <sup>-1</sup> , Q2D)	> 100% <sup>[b]</sup>
TMD-8 (14 mg kg <sup>-1</sup> , Q2D)	75%

[a] In mice; TGI = tumor growth inhibition. [b] Tumor regression.

### Preclinical pharmacokinetics

The preclinical pharmacokinetics of copanlisib (**39i**) has been presented in detail elsewhere.<sup>[42]</sup> Copanlisib has a high plasma-free fraction across all species tested (42.5% in male Wistar

rats, 27.6% in male CD1 mice, 42.4% in female Beagle dogs and 15.8% in male humans). Furthermore, copanlisib has low permeability in the Caco2 assay, with a  $P_{app}$  value for the apical (A) to basal (B) direction of  $56.9 \pm 2.91 \text{ nm s}^{-1}$  at  $10 \mu\text{M}$  in the absence of a P-glycoprotein (P-gp) inhibitor. Copanlisib was characterized as a substrate of the efflux transporters P-gp and BCRP. In vitro studies with different cell lines, P-gp (IC<sub>50</sub>:  $7 \mu\text{M}$  for digoxin and  $7.6 \mu\text{M}$  for dipyrindamole) and BCRP (IC<sub>50</sub>:  $11.5 \mu\text{M}$  for topotecan) mediated transport was inhibited.

The pharmacokinetic profile of copanlisib was evaluated following administration of single or multiple intravenous doses to nude rats. The volume of distribution ( $V_{ss}$ ) was very high in all species investigated including mouse, rat, dog and monkey ( $V_{ss} = 7\text{--}32 \text{ L kg}^{-1}$ ). In rats and dogs, the whole-blood clearance (CL) was  $2.8$  and  $0.74 \text{ L (h kg)}^{-1}$ , respectively, and thus was 66 and 35%, respectively, relative to hepatic blood flow. Pharmacokinetics was not dependent on sex and no relevant drug accumulation was observed after repeated administration (every second day  $\times 5$ ), suggesting that there is no change in metabolic processes. Thus, the pharmacokinetic profile of copanlisib was supportive of initiating clinical studies.

## Conclusions

The discovery of the novel 2,3-dihydroimidazo[1,2-c]quinazoline scaffold has led to the development of potent and selective PI3K inhibitors which strongly bind at both at the hinge and the affinity pocket. During the course of optimization, compound **39i** (copanlisib, BAY 80-6946)<sup>[42]</sup> was identified as having met program criteria, and as having excellent efficacy in in vitro and in vivo studies.<sup>[43]</sup> Copanlisib was selected for clinical development, and is currently in phase III trials for the treatment of non-Hodgkin lymphoma (NHL), both as monotherapy (CHRONOS-2: NCT02369016) and in combination with rituximab (CHRONOS-3: NCT02367040) or rituximab-based chemotherapy (CHRONOS-4: NCT02626455).

## Experimental Section

**Biochemical IC<sub>50</sub> assays:**<sup>[42]</sup> p110 $\alpha$ , p100 $\beta$  and p110 $\gamma$  activities were measured by the inhibition of 33P incorporation into phosphatidylinositol (PI) in 384-well MaxiSorp® plates coated with PI (2  $\mu\text{g}$  per well) and phosphatidylserine (PS) (1:1 molar ratio). Each PI3K isoform assay contained: reaction buffer (9  $\mu\text{L}$  of MOPSO (50 mM, pH 7.0), NaCl (100 mM), MgCl<sub>2</sub> (4 mM), BSA (0.1%)) containing His-tagged N-terminal truncated ( $\Delta$ N 1–108) p110 $\alpha$  or p110 $\beta$  protein (7.5 ng), or purified human p110 $\gamma$  protein (25 ng) (Alexis Biochemicals). The reaction was started by adding ATP solution containing  $20 \mu\text{Ci mL}^{-1}$  [<sup>33</sup>P]ATP (5  $\mu\text{L}$ , 40  $\mu\text{M}$ ). After incubation for 2 h at RT, the reaction was terminated by addition of EDTA solution (5  $\mu\text{L}$ , 25 mM). The plates were washed and Ultima Gold™ scintillation cocktail (25  $\mu\text{L}$ ) was then added. The radioactivity incorporated into the immobilized PI substrate was determined with



a BetaPlate Liquid Scintillation Counter. Each IC<sub>50</sub> value reported is the mean of a minimum of two experiments.

**General procedures:** Air- and moisture-sensitive liquids and solutions were transferred via syringe or cannula, and introduced into reaction vessels through rubber septa. Commercial grade reagents and solvents were used without further purification. The term 'concentrated under reduced pressure' refers to use of a Büchi rotary evaporator at approximately 15 mmHg. Thin-layer chromatography was performed on precoated glass-backed silica gel 60A F<sub>254</sub> 250 µm plates.

**NMR:** Routine 1D-NMR spectroscopy was performed on either a 300 or 400 MHz Varian Mercury Plus spectrometer, except where otherwise indicated. Samples were dissolved in deuterated solvents. Chemical shifts, recorded on the ppm scale, are referenced to the appropriate solvent signals (e.g., for <sup>1</sup>H NMR spectra: [D<sub>6</sub>]DMSO, 2.49 ppm; CDCl<sub>3</sub>, 7.26 ppm).

**GC-MS:** Electron-impact mass spectra (EI-MS) were obtained using a Hewlett Packard 5973 mass spectrometer equipped with a Hewlett Packard 6890 gas chromatograph with a J&W HP-5 column (30 m × 0.32 mm, 0.25 µm). The ion source was maintained at 250 °C and spectra were scanned from 50–550 amu at 0.34 s per scan.

**Synthesis:** Compounds **5–21**, **38a–38g**, **40** and **41** were synthesized as previously reported.<sup>[37]</sup>

**4-Formyl-2-methoxy-3-nitrophenyl acetate (23):** Fuming nitric acid (2.2 L) under nitrogen was cooled to 0 °C at which time vanillin acetate (**22**; 528 g, 2.7 mol) was added portionwise, keeping the internal temperature below 10 °C. After 2 h the resulting mixture was poured into ice with stirring. The slurry was filtered and the resulting solids were washed with water (3 × 100 mL) and air-dried. After 2 d the solids were heated in CH<sub>2</sub>Cl<sub>2</sub> (3000 mL) until complete dissolution. The solution was allowed to cool to RT while hexane (3000 mL) was added dropwise. The solids were collected by filtration, washed with hexane (500 mL) and air-dried to give **23** (269 g, 41%); <sup>1</sup>H NMR ([D<sub>6</sub>]DMSO): δ = 2.40 (s, 3H), 3.87 (s, 3H), 7.75 (d, 1H), 7.94 (d, 1H), 9.90 ppm (s, 1H).

**4-Hydroxy-3-methoxy-2-nitrobenzaldehyde (24):** A mixture of acetate **23** (438 g, 1.8 mol) and K<sub>2</sub>CO<sub>3</sub> (506 g, 3.7 mol) in MeOH (4 L) was stirred at RT for 16 h. Then, the reaction mixture was concentrated under reduced pressure to afford a viscous oil. The residue was dissolved in water, and the solution was acidified using HCl (2 N) and extracted with EtOAc. The organic layer was washed with saturated aqueous NaCl solution, dried (MgSO<sub>4</sub>) and filtered. The solution was concentrated under reduced pressure to 1/3 volume and the resulting solid was collected by filtration to give **24** (317 g, 88%); <sup>1</sup>H NMR ([D<sub>6</sub>]DMSO): δ = 3.82 (s, 3H), 7.19 (d, 1H), 7.68 (d, 1H), 9.69 ppm (s, 1H); MS (ESI+) *m/z*: 198 [M + H]<sup>+</sup>.

**4-(Benzyloxy)-3-methoxy-2-nitrobenzaldehyde (25):** Phenol **24** (155 g, 786 mmol) was dissolved in DMF (1500 mL) and the stirred solution was treated with K<sub>2</sub>CO<sub>3</sub> (217 g, 1.57 mol) followed by benzyl bromide (161 g, 0.94 mol). The reaction mixture was stirred for 16 h, then concentrated under reduced pressure and separated between water (2 L) and EtOAc (2 L). The organic layer was washed with saturated aqueous NaCl solution (3 × 2 L), dried (Na<sub>2</sub>SO<sub>4</sub>) and concentrated under reduced pressure. The resulting solids were triturated with Et<sub>2</sub>O (1 L) to give **25** (220 g, 97%); <sup>1</sup>H NMR ([D<sub>6</sub>]DMSO): δ = 3.05 (s, 3H), 5.36 (s, 2H), 7.39 (m, 3H), 7.49 (m, 1H), 7.51 (m, 1H), 7.58 (d, 1H), 7.87 (d, 1H), 9.77 ppm (s, 1H); MS (ESI+) *m/z*: 288 [M + H]<sup>+</sup>.

**4-(Benzyloxy)-3-methoxy-2-nitrobenzonitrile (26):** Iodine (272 g, 1.1 mol) was added to a mixture of aldehyde **25** (220 g, 766 mmol) and ammonium hydroxide (28% solution, 3 L) dissolved in THF (5 L). After 16 h the reaction mixture was treated with sodium sulfite (49 g, 383 mmol), then concentrated under reduced pressure to afford a thick slurry. The slurry was filtered, washed with water (250 mL) and air-dried to give nitrile **26** (206 g, 95%); <sup>1</sup>H NMR ([D<sub>6</sub>]DMSO): δ = 3.91 (s, 3H), 5.35 (s, 2H), 7.40 (m, 3H), 7.49 (m, 2H), 7.59 (d, 1H), 7.89 ppm (d, 1H).

**2-Amino-4-(benzyloxy)-3-methoxybenzonitrile (27):** A degassed solution of nitrobenzonitrile **26** (185 g, 651 mmol) in glacial acetic acid (3500 mL) and water (10 mL) was cooled to 5 °C and treated with iron powder (182 g, 3.25 mol). After 3 d at RT the reaction mixture was filtered through Celite®, and the filtrate was concentrated under reduced pressure. The oil, thus obtained, was treated with saturated aqueous NaCl solution, neutralized with sodium bicarbonate solution and extracted with CH<sub>2</sub>Cl<sub>2</sub>. The resulting emulsion was filtered through Celite®, after which the organic layer was separated, washed with saturated aqueous NaCl solution, dried (Na<sub>2</sub>SO<sub>4</sub>) and concentrated under reduced pressure to give **27** (145 g, 88%); <sup>1</sup>H NMR ([D<sub>6</sub>]DMSO): δ = 3.68 (s, 3H), 5.15 (s, 2H), 5.69 (s, 2H), 6.47 (d, 1H), 7.15 (d, 1H), 7.32–7.44 ppm (m, 5H).

**3-(Benzyloxy)-6-(4,5-dihydro-1H-imidazol-2-yl)-2-methoxyaniline (28):** A mixture of nitrile **27** (144 g, 566 mmol) and sulfur (55 g, 1.7 mol) in ethylenediamine (800 mL) was degassed for 30 min, then heated at 100 °C. After 16 h the reaction mixture was cooled to RT and then filtered. The filtrate was concentrated under reduced pressure, diluted with saturated sodium bicarbonate solution and extracted with EtOAc. The organic layer was washed with saturated aqueous NaCl solution, dried (Na<sub>2</sub>SO<sub>4</sub>), filtered and concentrated under reduced pressure. The resulting solids were recrystallized from EtOAc/hexane giving **28** (145 g, 86%); <sup>1</sup>H NMR ([D<sub>6</sub>]DMSO): δ = 3.33 (s, 2H), 3.67 (s, 3H), 3.76 (brs, 2H), 5.11 (s, 2H), 6.32 (d, 1H), 6.64 (m, 1H), 6.92 (m, 2H), 7.14 (d, 1H), 7.27–7.48 ppm (m, 5H).

**8-(Benzyloxy)-7-methoxy-2,3-dihydroimidazo[1,2-c]quinazolin-5-amine (29):** A mixture of amine **28** (100 g, 336 mmol) and triethylamine (TEA) (188 mL) in CH<sub>2</sub>Cl<sub>2</sub> (3 L) was cooled to 0 °C and treated with cyanogen bromide (78.4 g, 740 mmol). The reaction mixture was stirred and allowed to warm to RT gradually. After 16 h it was diluted with saturated sodium bicarbonate solution and extracted with CH<sub>2</sub>Cl<sub>2</sub>. The organic layer was washed with saturated sodium bicarbonate solution followed by multiple washes with saturated aqueous NaCl solution. The organic layer was dried (Na<sub>2</sub>SO<sub>4</sub>) and concentrated under reduced pressure to give **29** (130 g, quant.); <sup>1</sup>H NMR ([D<sub>6</sub>]DMSO): δ = 3.81 (s, 3H), 4.13 (m, 2H), 4.32 (m, 2H), 5.31 (s, 2H), 7.30–7.48 ppm (m, 7H); MS (ESI+) *m/z*: 323 [M + H]<sup>+</sup>.

**N-[8-(Benzyloxy)-7-methoxy-2,3-dihydroimidazo[1,2-c]quinazolin-5-yl]nicotinamide (30):** Amine **29** (21 g, 65 mmol) and nicotinic acid (12 g, 97.7 mmol) were suspended in DMF (240 mL). *N,N*-Diisopropylethylamine (DIPEA) (33.7 g, 260.4 mmol) and then (benzotriazol-1-yloxy)tripyrrolidinophosphonium hexafluorophosphate (PyBOP; 51 g, 97.7 mmol) were added and the resulting mixture was stirred with overhead stirring at RT for 3 d. The resultant precipitate was isolated by vacuum filtration. After repeated washing with EtOAc, the material was dried under reduced pressure with slight heating to give **30** (27.3 g, 98%); <sup>1</sup>H NMR ([D<sub>6</sub>]DMSO + 2 drops [D]TFA): δ = 3.78 (s, 3H), 4.04 (t, 2H), 4.36 (t, 2H), 5.18 (s, 2H), 7.16 (m, 6H), 7.27 (d, 1H), 7.37 (d, 1H), 7.82 (d, 1H), 7.89 (brm, 1H), 8.84 (d, 1H), 8.89 (brm, 1H), 9.32 ppm (s, 1H); MS (ESI+) *m/z*: 428 [M + H]<sup>+</sup>.

**N-(8-Hydroxy-7-methoxy-2,3-dihydroimidazo[1,2-c]quinazolin-5-yl)nicotinamide (31):** Benzyl ether **30** (20 g, 45.1 mmol) was added portionwise over 1 h to a round-bottom flask containing trifluoroacetic acid (TFA) (400 mL) precooled with an ice bath. The reaction mixture was heated at 60 °C and allowed to stir at this temperature for 17 h, at which time it was cooled to RT. Then, it was concentrated under reduced pressure. The resulting residue was taken up in CH<sub>2</sub>Cl<sub>2</sub> and hexane, and the solution was concentrated under reduced pressure. The material thus obtained was dissolved in MeOH/CH<sub>2</sub>Cl<sub>2</sub> (1:1, 250 mL) and concentrated under reduced pressure. The resulting solids were dried overnight under reduced pressure with low heat to give **31** (bis-TFA salt; 17.3 g, 66%): <sup>1</sup>H NMR ([D<sub>6</sub>]DMSO + 2 drops [D]TFA): δ = 3.98 (s, 3H), 4.21 (m, 2H), 4.54 (m, 2H), 7.17 (d, 1H), 7.59 (m, 1H), 7.85 (d, 1H), 8.53 (d, 1H), 8.78 (d, 1H), 9.38 (s, 1H), 12.21 (brs, 1H), 13.41 ppm (s, 1H); MS (ESI+) *m/z*: 338 [M+H]<sup>+</sup>; HRMS-ESI *m/z* [M+H]<sup>+</sup> calcd for C<sub>17</sub>H<sub>16</sub>N<sub>5</sub>O<sub>3</sub>: 338.1253, found: 338.1252.

**N-(7,8-Dimethoxy-2,3-dihydroimidazo[1,2-c]quinazolin-5-yl)nicotinamide (32a):**<sup>[32]</sup> Potassium *tert*-butylate (69.9 mg, 623 μmol) was added to a slurry of phenol **31** (210 mg, 623 μmol) in DMF (5 mL), followed by dimethyl sulfate (12 μL, 120 μmol). The reaction mixture was stirred at RT for 2 h. Dimethyl sulfate (12 μL, 120 μmol) was again added and the reaction mixture was stirred at RT for a further 2 h, then concentrated under reduced pressure and dissolved in CH<sub>2</sub>Cl<sub>2</sub>/MeOH (1:1, 5 mL). Potassium *tert*-butylate (69.9 mg, 623 μmol) and dimethyl sulfate (12 μL, 120 μmol) were again added. The reaction mixture was stirred at RT for 1 h, then concentrated under reduced pressure and purified by flash chromatography (MeOH/EtOAc) to give **32a** (140 mg, 65%): <sup>1</sup>H NMR ([D<sub>6</sub>]DMSO): δ = 4.00 (s, 4H), 4.06 (s, 3H), 4.25–4.33 (m, 2H), 4.56–4.64 (m, 2H), 7.53 (d, 1H), 8.03–8.13 (m, 2H), 9.05 (d, 2H), 9.56 ppm (s, 1H); MS (ESI+) *m/z*: 352 [M+H]<sup>+</sup>; HRMS-ESI *m/z* [M+H]<sup>+</sup> calcd for C<sub>18</sub>H<sub>18</sub>N<sub>5</sub>O<sub>3</sub>: 352.1410, found: 352.1408.

**N-(8-Ethoxy-7-methoxy-2,3-dihydroimidazo[1,2-c]quinazolin-5-yl)nicotinamide (32b):** Ethyl methanesulfonate (68 μL, 0.66 mmol) was added to a suspension of phenol **31** (TFA salt; 150 mg, 0.33 mmol) and Cs<sub>2</sub>CO<sub>3</sub> (433 mg, 1.33 mmol) in DMF (7 mL). The reaction mixture was stirred at RT for 48 h, then concentrated under reduced pressure. The crude mixture was purified by flash column chromatography (0–2% MeOH/CH<sub>2</sub>Cl<sub>2</sub>) to give **32b** (97 mg, 80%): <sup>1</sup>H NMR (500 MHz, [D<sub>6</sub>]DMSO + 3 drops [D]TFA): δ = 1.47 (t, 3H), 4.04 (s, 3H), 4.28–4.33 (m, 2H), 4.37 (q, 2H), 4.59–4.64 (m, 2H), 7.52 (d, 1H), 8.07 (dd, 1H), 8.09 (d, 1H), 9.02–9.09 (m, 2H), 9.58 ppm (s, 1H); HRMS-ESI *m/z* [M+H]<sup>+</sup> calcd for C<sub>19</sub>H<sub>20</sub>N<sub>5</sub>O<sub>3</sub>: 366.1566, found: 366.1569.

**N-(8-Isobutoxy-7-methoxy-2,3-dihydroimidazo[1,2-c]quinazolin-5-yl)nicotinamide (32c):** A suspension of phenol **31** (bis-TFA salt; 150 mg, 265 μmol) and Cs<sub>2</sub>CO<sub>3</sub> (346 mg, 1.06 mmol) in DMF (5 mL) was stirred at RT for 1.5 h. 2-Methylpropan-1-ol (51 μL, 560 μmol) and TEA (78 μL, 560 μmol) were solubilized in anhydrous DMF (2 mL), and this solution was slowly added to the previous suspension. The reaction mixture was stirred at RT for 48 h. Cs<sub>2</sub>CO<sub>3</sub> (346 mg, 1.06 mmol) was again added to the mixture which was stirred for an additional 48 h at 50 °C. The reaction mixture was cooled to RT, then concentrated under reduced pressure. The crude mixture was purified by flash column chromatography (0–2% MeOH/CH<sub>2</sub>Cl<sub>2</sub>) to give **32c** (90 mg, 86%): <sup>1</sup>H NMR (500 MHz, [D<sub>6</sub>]DMSO + 3 drops [D]TFA): δ = 1.06 (d, 6H), 2.16 (dt, 1H), 4.05 (s, 3H), 4.08 (d, 2H), 4.25–4.32 (m, 2H), 4.56–4.63 (m, 2H), 7.51 (d, 1H), 7.83 (dd, 1H), 8.07 (d, 1H), 8.80 (d, 1H), 8.94 (dd, 1H), 9.49 ppm (d, 1H); HRMS-ESI *m/z* [M+H]<sup>+</sup> calcd for C<sub>21</sub>H<sub>24</sub>N<sub>5</sub>O<sub>3</sub>: 394.1879, found: 394.1880.

***tert*-Butyl [3-({7-methoxy-5-[(pyridin-3-ylcarbonyl)amino]-2,3-dihydroimidazo[1,2-c]quinazolin-8-yl)oxy}propyl]carbamate (32d')**: Phenol **31** (1.5 g, 4.4 mmol) was dissolved in DMF (50 mL) containing a few drops of water. Cs<sub>2</sub>CO<sub>3</sub> (7.24 g, 22.2 mmol) and NaI (0.80 g, 5.3 mmol) were added, followed by *tert*-butyl (3-bromopropyl)carbamate (3.18 g, 13.3 mmol). The mixture was stirred at 100 °C overnight. After the mixture was cooled to RT, the volatiles were removed under reduced pressure. The residue was diluted with MeOH/CH<sub>2</sub>Cl<sub>2</sub> (1:9), and solids were removed by filtration. The filtrate was concentrated and purified by silica gel flash column chromatography (0–10% MeOH/CH<sub>2</sub>Cl<sub>2</sub>) to afford **32d'** (1.13 g, 51%): <sup>1</sup>H NMR ([D<sub>6</sub>]DMSO + 2 drops [D]TFA): δ = 1.37 (s, 9H), 1.94 (m, 2H), 3.15 (t, 2H), 4.03 (s, 3H), 4.26 (m, 4H), 4.57 (m, 2H), 6.96 (brt, 1H), 7.47 (d, 1H), 7.82 (m, 1H), 8.03 (d, 1H), 8.79 (m, 1H), 8.91 (m, 1H), 9.46 ppm (m, 1H).

**N-[8-(3-Aminopropoxy)-7-methoxy-2,3-dihydroimidazo[1,2-c]quinazolin-5-yl]nicotinamide hydrotrifluoroacetate (32d):** Carbamate **32d'** (1.2 g, 2.3 mmol) was dissolved in a mixture of TFA (6 mL) and CH<sub>2</sub>Cl<sub>2</sub> (24 mL). The mixture was stirred at RT overnight, then concentrated under reduced pressure to afford a viscous yellow oil. Acetonitrile was added to the mixture, and the desired product **32d** was isolated by vacuum filtration as a white solid (TFA salt; 0.55 g, 47%): <sup>1</sup>H NMR ([D<sub>6</sub>]DMSO + 2 drops [D]TFA): δ = 2.13 (m, 2H), 3.02 (m, 2H), 4.01 (s, 3H), 4.25 (m, 2H), 4.35 (t, 2H), 4.57 (m, 2H), 7.45 (d, 1H), 7.73 (m, 1H), 7.92 (brm, 2H), 8.06 (d, 1H), 8.69 (m, 1H), 8.87 (m, 1H), 9.43 ppm (m, 1H).

**N-[8-[3-(Dimethylamino)propoxy]-7-methoxy-2,3-dihydroimidazo[1,2-c]quinazolin-5-yl]nicotinamide (32e):** A suspension of phenol **31** (bis-TFA salt; 2.00 g, 3.54 mmol), 3-chloro-*N,N*-dimethylpropan-1-amine hydrochloride (839 mg, 5.31 mmol) and Cs<sub>2</sub>CO<sub>3</sub> (5.76 g, 17.7 mmol) in DMF (40 mL) was heated in a sealed tube at 120 °C for 3 h. The reaction mixture was then cooled to RT and concentrated under reduced pressure. Ice was added to the mixture and the precipitate was collected by filtration and dried under reduced pressure to give **32e**, without further purification (1 g, 67%): <sup>1</sup>H NMR (500 MHz, [D<sub>6</sub>]DMSO + 3 drops [D]TFA): δ = 2.26 (dd, 1H), 2.87 (s, 3H), 3.27–3.32 (m, 2H), 4.05 (s, 3H), 4.27–4.32 (m, 2H), 4.37 (t, 2H), 4.61 (dd, 2H), 7.50 (d, 1H), 7.86–7.92 (m, 1H), 8.11 (dd, 1H), 8.83–8.89 (m, 1H), 8.96–9.00 (m, 1H), 9.52 ppm (s, 1H); MS (ESI+) *m/z*: 423 [M+H]<sup>+</sup>; HRMS-ESI *m/z* [M+H]<sup>+</sup> calcd for C<sub>22</sub>H<sub>27</sub>N<sub>6</sub>O<sub>3</sub>: 423.2145, found: 423.2145.

**N-[7-Methoxy-8-[3-(piperidin-1-yl)propoxy]-2,3-dihydroimidazo[1,2-c]quinazolin-5-yl]nicotinamide (32f):** Phenol **31** (bis-TFA salt; 150 mg, 265 μmol) and 1-(3-chloropropyl)piperidine hydrochloride (158 mg, 796 μmol) were added to a suspension of NaH (41.4 mg, 1.72 mmol) in DMF (4 mL). The reaction mixture was stirred at 50 °C for 2 h, then NaH (41.4 mg, 1.72 mmol) was added again. After 2 h further NaH (41.4 mg, 1.72 mmol) was added, along with 1-(3-chloropropyl)piperidine hydrochloride (158 mg, 796 μmol). The reaction mixture was stirred at 50 °C overnight, then cooled to RT and carefully quenched by the addition of water. The organic phase was extracted with CH<sub>2</sub>Cl<sub>2</sub> and the extract was concentrated under reduced pressure; trituration with EtOAc gave **32f** (45 mg, 36%): <sup>1</sup>H NMR (500 MHz, [D<sub>6</sub>]DMSO + 3 drops [D]TFA): δ = 1.42 (d, 1H), 1.64–1.76 (m, 3H), 1.85 (d, 2H), 2.28 (dd, 2H), 2.92–3.00 (m, 2H), 3.23–3.29 (m, 2H), 3.53 (d, 2H), 4.04 (s, 3H), 4.25–4.31 (m, 2H), 4.37 (t, 2H), 4.57–4.63 (m, 2H), 7.49 (d, 1H), 7.77 (dd, 1H), 8.11 (d, 1H), 8.73 (d, 1H), 8.91 (dd, 1H), 9.47 ppm (s, 1H); HRMS-ESI *m/z* [M+H]<sup>+</sup> calcd for C<sub>25</sub>H<sub>31</sub>N<sub>6</sub>O<sub>3</sub>: 463.2458, found: 463.2455.

**4-(3-Chloropropyl)morpholine hydrochloride (32g')**: To a solution of 1-bromo-3-chloropropane (45 g, 0.29 mol) in toluene (100 mL), morpholine (38 g, 0.44 mol) was added. The solution was stirred at 84 °C for 3 h, during which time a precipitate formed. After the solution was cooled to RT, the precipitate was isolated by vacuum filtration and washed with Et<sub>2</sub>O, and the solid was discarded. The mother liquor was acidified with HCl (4 N) in dioxane (72 mL, 0.29 mol), which resulted in the desired product precipitating as the HCl salt. The volatiles were removed under reduced pressure, and the resultant solid was dried to give **32g'** (HCl salt; 53 g, 90%): <sup>1</sup>H NMR ([D<sub>6</sub>]DMSO): δ = 2.21 (m, 2H), 3.03 (m, 2H), 3.15 (m, 2H), 3.39 (m, 2H), 3.74 (t, 2H), 3.77–3.94 (m, 4H), 11.45 ppm (brs, 1H).

**N-[7-Methoxy-8-[3-(morpholin-4-yl)propoxy]-2,3-dihydroimidazo[1,2-c]quinazolin-5-yl]nicotinamide (32g)**: Phenol **31** (bis-TFA salt; 5.00 g, 8.84 mmol) was solubilized in DMF (81 mL) and Cs<sub>2</sub>CO<sub>3</sub> (14.4 g, 44.2 mmol) was added. The mixture was stirred at RT for 1.5 h, then 4-(3-chloropropyl)morpholine hydrochloride (**32g'**; 2.65 g, 13.3 mmol) was added. The reaction mixture was stirred at 60 °C for 20 h, then the crude mixture was concentrated under reduced pressure. The crude material was stirred in water (200 mL) for 1 h, and the suspension was filtered and dried under reduced pressure to give **32g** (3.26 g, 79%): <sup>1</sup>H NMR ([D<sub>6</sub>]DMSO + 2 drops [D]TFA): δ = 2.25 (m, 2H), 3.18 (m, 2H), 3.31 (m, 2H), 3.52 (m, 2H), 3.65 (brt, 2H), 4.00 (s, 3H), 4.04 (m, 2H), 4.23 (m, 2H), 4.34 (brt, 2H), 4.54 (m, 2H), 7.43 (d, 1H), 8.04 (d, 1H), 9.01 ppm (s, 2H); MS (ESI+) *m/z*: 465 [M+H]<sup>+</sup>; HRMS-ESI *m/z* [M+H]<sup>+</sup> calcd for C<sub>24</sub>H<sub>29</sub>N<sub>6</sub>O<sub>4</sub>: 465.2250, found: 465.2249.

**N-[7-Methoxy-8-[2-(morpholin-4-yl)ethoxy]-2,3-dihydroimidazo[1,2-c]quinazolin-5-yl]nicotinamide (32h)**: Phenol **31** (1.34 g, 3.97 mmol) was solubilized in DMF (50 mL) and NaH (60% in mineral oil; 794 mg, 19.9 mmol) was added. The reaction mixture was stirred at RT for 20 min, then 4-(2-chloroethyl)morpholine hydrochloride (1.48 g, 7.94 mmol) was added in one portion. The reaction mixture was stirred at 100 °C for 16 h, then was cooled to RT and concentrated under reduced pressure. The crude material was solubilized in chloroform and the solution was washed with water. The organic phase was dried (Na<sub>2</sub>SO<sub>4</sub>), filtered and concentrated under reduced pressure. The crude material was purified by flash column chromatography to give **32h** (400 mg, 22%): HRMS-ESI *m/z* [M+H]<sup>+</sup> calcd for C<sub>23</sub>H<sub>27</sub>N<sub>6</sub>O<sub>4</sub>: 451.2094, found: 451.2097.

**N-[8-(4-Chlorobutoxy)-7-methoxy-2,3-dihydroimidazo[1,2-c]quinazolin-5-yl]nicotinamide (32i')**: A mixture of 1-bromo-4-chlorobutane (57.0 mg, 333 μmol), phenol **31** (102 mg, 302 μmol) and Cs<sub>2</sub>CO<sub>3</sub> (296 mg, 907 μmol) in DMF (10 mL) was stirred at RT for 2 d. Then, the reaction mixture was filtered and the filtrate was concentrated under reduced pressure. The crude material was purified by flash column chromatography to give **32i'** (60 mg, 48%).

**N-[7-Methoxy-8-[4-(morpholin-4-yl)butoxy]-2,3-dihydroimidazo[1,2-c]quinazolin-5-yl]nicotinamide (32i)**: A mixture of chloride **32i'** (50.0 mg, 117 μmol) and morpholine (1.0 mL, 11.4 mmol) in dioxane (4 mL) was held at reflux for 18 h. The reaction mixture was then cooled to RT and concentrated under reduced pressure. Water was added to the mixture, and the precipitate was collected by filtration and washed with a mixture of MeOH/Et<sub>2</sub>O to give **32i** (14 mg, 25%), without further purification.

**N-[7-Hydroxy-8-[3-(morpholin-4-yl)propoxy]-2,3-dihydroimidazo[1,2-c]quinazolin-5-yl]nicotinamide (33)**: Methyl ether **32g** (1.0 g, 2.15 mmol) in *N*-methyl-2-pyrrolidinone (20 mL) was heated at 100 °C and Na<sub>2</sub>S (0.84 g, 10.76 mmol) was added portionwise. The reaction mixture was heated at 160 °C for 10 min, then cooled

to RT and concentrated under reduced pressure. The resulting slurry was diluted with water (100 mL) and the mixture was adjusted to pH 7 by the slow addition of aqueous HCl (1 N); the mixture was stirred for 2 h. The solid was collected via vacuum filtration and washed with water (50 mL), and finally triturated with CH<sub>2</sub>Cl<sub>2</sub>/heptane (1:1, 10 mL). High-vacuum drying overnight gave **33** (0.49 g, 51%): <sup>1</sup>H NMR ([D<sub>6</sub>]DMSO + 2 drops [D]TFA): δ = 2.14–2.26 (m, 2H), 3.03–3.17 (m, 2H), 3.32–3.54 (m, 4H), 3.60–3.72 (m, 2H), 3.95–4.05 (m, 2H), 4.18–4.35 (m, 4H), 4.51–4.64 (m, 2H), 7.38 (d, 1H), 7.68 (dd, 1H), 7.82 (d, 1H), 8.63 (s, 1H), 8.84 (dd, 1H), 9.42 (s, 1H), 13.39 ppm (s, 1H); MS (ESI+) *m/z*: 451 [M+H]<sup>+</sup>.

**N-[8-[3-(Morpholin-4-yl)propoxy]-7-propoxy-2,3-dihydroimidazo[1,2-c]quinazolin-5-yl]nicotinamide (34a)**: Phenol **33** (TFA salt; 370 mg, 655 μmol) and K<sub>2</sub>CO<sub>3</sub> (452 mg, 3.28 mmol) were suspended in DMF (3 mL), and 1-iodopropane (130 μL, 1.3 mmol) was added. The reaction mixture was stirred at RT for 5 h, then the volatiles were removed under reduced pressure. The residue was purified by flash chromatography (0–7% MeOH/CH<sub>2</sub>Cl<sub>2</sub>) to give **34a** as an oil that solidified on standing. Trituration with cold acetone/MeOH (9:1) gave a white solid (65 mg, 20%): MS (ESI+) *m/z*: 493.1 [M+H]<sup>+</sup>; HRMS-ESI *m/z* [M+H]<sup>+</sup> calcd for C<sub>26</sub>H<sub>33</sub>N<sub>6</sub>O<sub>4</sub>: 493.2563, found: 493.2559.

**N-[7-(Allyloxy)-8-[3-(morpholin-4-yl)propoxy]-2,3-dihydroimidazo[1,2-c]quinazolin-5-yl]nicotinamide (34b)**: To an orange-brown solution of phenol **33** (50.0 mg, 111 μmol) in DMF (2.0 mL) K<sub>2</sub>CO<sub>3</sub> (5 m; 62 μL, 330 μmol) was added, followed by allyl bromide (14 μL, 170 μmol). The resulting pale-yellow mixture was stirred at RT for 1 d. Then, the reaction mixture was concentrated under reduced pressure. The residue was taken up in CH<sub>2</sub>Cl<sub>2</sub> and a small volume of MeOH, and the slurry was filtered. The filtrate was purified by flash chromatography (5–10% MeOH/CH<sub>2</sub>Cl<sub>2</sub>) to give **34b** as a white solid (10 mg, 18%): MS (ESI+) *m/z*: 491 [M+H]<sup>+</sup>.

**N-[7-Isobutoxy-8-[3-(morpholin-4-yl)propoxy]-2,3-dihydroimidazo[1,2-c]quinazolin-5-yl]nicotinamide (34c)**: To a slurry of phenol **33** (100 mg, 222 μmol) in DMF (4.0 mL) was added NaH (16 mg, 670 μmol); gas evolution was observed upon the dissolution of **33**. After 30 min, 1-bromo-2-methylpropane (38 mg, 277 μmol) was added. The resulting orange solution was stirred at RT for 17 h. Then, further 1-bromo-2-methylpropane (40 mg, 292 μmol) was added and the mixture was stirred for 3 h. Water was added, and the mixture was adjusted to pH 7 with a few drops of aqueous HCl (1 N). The mixture was extracted with CH<sub>2</sub>Cl<sub>2</sub> and the combined extracts were dried (MgSO<sub>4</sub>) and concentrated under reduced pressure. Purification by flash chromatography (5–10% MeOH/CH<sub>2</sub>Cl<sub>2</sub>) gave **34c** as a white solid (30 mg, 26%): MS (ESI+) *m/z*: 507 [M+H]<sup>+</sup>.

**N-[7-(Cyclohexylmethoxy)-8-[3-(morpholin-4-yl)propoxy]-2,3-dihydroimidazo[1,2-c]quinazolin-5-yl]nicotinamide (34d)**: A slurry of phenol **33** (74.0 mg, 164 μmol) in *N,N*-dimethylacetamide (2 mL) was treated with NaH (60% in mineral oil; 13.1 mg, 329 μmol) for 30 min while being stirred vigorously. To the resulting solution was added (bromomethyl)cyclohexane (37 μL, 250 μmol) and Ag<sub>2</sub>CO<sub>3</sub> (67.9 mg, 246 μmol); the mixture was stirred overnight and then heated at 100 °C for 2 h. Dilution with water (20 mL) resulted in a deep purple mixture which was filtered through a pad of Celite®. The pad was washed with water and CH<sub>2</sub>Cl<sub>2</sub>. The filtrate was separated and the aqueous layer was extracted with CH<sub>2</sub>Cl<sub>2</sub>. The combined organic layers were concentrated to dryness under reduced pressure. The residue was dissolved in CH<sub>2</sub>Cl<sub>2</sub> and purified by flash chromatography (MeOH/EtOAc 2:8 to MeOH/CH<sub>2</sub>Cl<sub>2</sub> 5:95) to give **34d** as a white solid (10 mg, 11%): MS (ESI+) *m/z*: 547 [M+H]<sup>+</sup>;



HRMS-ESI  $m/z$   $[M+H]^+$  calcd for  $C_{30}H_{39}N_6O_4$ : 547.3033, found: 547.3033.

**N-[8-[3-(Morpholin-4-yl)propoxy]-7-[(tetrahydro-2H-pyran-4-yl)-methoxy]-2,3-dihydroimidazo[1,2-c]quinazolin-5-yl]nicotinamide (34e):** To a slurry of phenol **33** (63.0 mg, 140  $\mu$ mol) in DMF (2.0 mL) was added NaH (60% in mineral oil; 8 mg, 210  $\mu$ mol). After 30 min 4-(bromomethyl)tetrahydro-2H-pyran (27  $\mu$ L, 210  $\mu$ mol) was added. The resulting orange solution was stirred at RT for 17 h. Then, further 4-(bromomethyl)tetrahydro-2H-pyran (27  $\mu$ L, 210  $\mu$ mol) was added and the mixture was stirred for 3 h. Water was added and the mixture was adjusted to pH 7 with a few drops of aqueous HCl (1 N). The mixture was extracted with  $CH_2Cl_2$  and the combined extracts were dried, filtered and concentrated under reduced pressure. Purification by flash chromatography (5–10% MeOH/ $CH_2Cl_2$ ) gave **34e** as a white solid (20 mg, 26%); MS (ESI+)  $m/z$ : 549  $[M+H]^+$ .

**N-[8-[3-(Morpholin-4-yl)propoxy]-7-[(pyridin-4-yl)methoxy]-2,3-dihydroimidazo[1,2-c]quinazolin-5-yl]nicotinamide (34f):** To a slurry of phenol **33** (100 mg, 222  $\mu$ mol) in DMF (2.0 mL), NaH (60% in mineral oil; 27 mg, 670  $\mu$ mol) was added; gas evolution was observed upon the dissolution of **33**. After 20 min, 4-(chloromethyl)pyridine hydrochloride (1:1; 54.6 mg, 333  $\mu$ mol) was added. The resulting orange mixture was stirred at RT; after 2 h a thick slurry formed. Stirring was continued overnight. Then, water was added and the mixture was adjusted to pH 7 with a few drops of aqueous HCl (1 N). The slurry was filtered to give **34f** as a white solid (40 mg, 35%);  $^1H$  NMR (500 MHz,  $[D_6]DMSO + 3$  drops  $[D]TFA$ ):  $\delta$  = 2.22–2.29 (m, 2H), 3.08–3.16 (m, 2H), 3.28–3.33 (m, 2H), 3.50 (d, 2H), 3.70 (t, 2H), 4.01 (d, 2H), 4.30 (t, 2H), 4.41 (t, 2H), 4.61 (t, 2H), 5.64 (brs, 2H), 7.56 (d, 1H), 7.81–7.92 (m, 1H), 8.17 (d, 1H), 8.28 (brs, 2H), 8.75–8.89 (m, 1H), 8.93–9.02 (m, 1H), 9.11 (brs, 2H), 9.49 ppm (brs, 1H); MS (ESI+)  $m/z$ : 542  $[M+H]^+$ .

**5-Amino-7-methoxy-2,3-dihydroimidazo[1,2-c]quinazolin-8-ol bis(trifluoroacetate) (35):** Amine **29** (30 g, 93 mmol) was added portionwise over 1 h to a round-bottom flask containing TFA (400 mL) precooled with an ice bath. The reaction mixture was heated at 60 °C and allowed to stir at this temperature for 17 h, at which time it was cooled to RT and then concentrated under reduced pressure. The resulting residue was taken up in  $CH_2Cl_2$  and hexanes, and concentrated under reduced pressure. The material thus obtained was dissolved in MeOH/ $CH_2Cl_2$  (1:1, 250 mL) and concentrated under reduced pressure. The resulting solid was dried overnight under reduced pressure with low heat to give **35** (44.7 g, quant.);  $^1H$  NMR ( $[D_6]DMSO$ ):  $\delta$  = 3.64 (s, 3H), 4.00 (m, 2H), 4.15 (brt, 2H), 6.87 (m, 1H), 7.61 ppm (m, 1H); MS (ESI+)  $m/z$ : 233  $[M+H]^+$ .

**7-Methoxy-8-[3-(morpholin-4-yl)propoxy]-2,3-dihydroimidazo[1,2-c]quinazolin-5-amine (36):** Phenol bis(trifluoroacetate) **35** (500 mg, 1.1 mmol) was dissolved in  $CH_2Cl_2$  (10 mL), and TEA (0.75 mL, 5.4 mmol) was added. The suspension was stirred at RT for 1.5 h, after which time 5-amino-7-methoxy-2,3-dihydroimidazo[1,2-c]quinazolin-8-ol hydrotrifluoroacetate was isolated. Thus prepared, this compound was dissolved in DMF (10 mL).  $Cs_2CO_3$  (1.41 g, 4.3 mmol) and chloride **32g'** (218 mg, 1.1 mmol) were added, and the mixture was stirred at 70 °C for 30 min. Additional chloride **32g'** (109 mg, 0.55 mmol) and  $Cs_2CO_3$  (350 mg, 1.1 mmol) were added, and stirring was continued for 1 h. Another portion of chloride **32g'** (109 mg, 0.55 mmol) was added, and the temperature was increased to 75 °C. After 3 h the reaction mixture was cooled to RT and filtered through a pad of Celite®, washing with MeOH and  $CH_2Cl_2$ . The filtrate was concentrated under reduced

pressure, dry-loaded onto silica gel and purified by chromatography ( $CH_2Cl_2$ /MeOH 95:5  $\rightarrow$   $CH_2Cl_2$ /MeOH  $\rightarrow$  9:1  $\rightarrow$   $CH_2Cl_2$ /2 M  $NH_3$  in MeOH 95:5  $\rightarrow$   $CH_2Cl_2$ /2 M  $NH_3$  in MeOH 85:15). The resultant oil was triturated with hexanes/EtOAc (1:1, 15 mL) to afford **36** as a solid (171 mg, 44%);  $^1H$  NMR ( $[D_6]DMSO$ ):  $\delta$  = 1.87 (m, 2H), 2.35 (m, 4H), 2.42 (t, 2H), 3.55 (m, 4H), 3.69 (s, 3H), 3.88 (m, 4H), 4.03 (t, 2H), 6.73 (m, 3H), 7.43 ppm (d, 1H); MS (ESI+)  $m/z$ : 360.3  $[M+H]^+$ .

**N-[7-Methoxy-8-[3-(morpholin-4-yl)propoxy]-2,3-dihydroimidazo[1,2-c]quinazolin-5-yl]-1,3-benzodioxole-5-carboxamide (39a):** To a vigorously stirred solution of amine **36** (50% purity; 154 mg, 214  $\mu$ mol) in DMF (2.0 mL) containing piperonylic acid (1,3-benzodioxole-5-carboxylic acid; 53.4 mg, 321  $\mu$ mol) and PyBOP (167 mg, 321  $\mu$ mol) was added DIPEA (150  $\mu$ L, 860  $\mu$ mol). After 20 min a thick slurry formed, and stirring was continued for 4 h. The slurry was filtered and the solid was washed with EtOAc to give **39a** as a white solid (60 mg, 55%);  $^1H$  NMR (500 MHz,  $[D_6]DMSO + 3$  drops  $[D]TFA$ ):  $\delta$  = 2.29 (dd, 2H), 3.14–3.21 (m, 2H), 3.33–3.37 (m, 2H), 3.54 (d, 2H), 3.70 (t, 2H), 4.01–4.06 (m, 2H), 4.03–4.04 (m, 3H), 4.22–4.27 (m, 2H), 4.36 (t, 2H), 4.52–4.57 (m, 2H), 6.15 (s, 2H), 7.03 (d, 1H), 7.44 (d, 1H), 7.67 (d, 1H), 7.88–7.93 (m, 1H), 8.05 ppm (d, 1H); MS (ESI+)  $m/z$ : 508  $[M+H]^+$ ; HRMS-ESI  $m/z$   $[M+H]^+$  calcd for  $C_{26}H_{30}N_5O_6$ : 508.2196, found: 508.2198.

**N-[7-Methoxy-8-[3-(morpholin-4-yl)propoxy]-2,3-dihydroimidazo[1,2-c]quinazolin-5-yl]-2,4-dimethyl-1,3-thiazole-5-carboxamide (39b):** Amine **36** (80% purity; 5.00 g, 11.1 mmol) was dissolved in DMF (1.2 mL), and 2,4-dimethyl-1,3-thiazole-5-carboxylic acid (2.62 g, 16.7 mmol), PyBOP (8.69 g, 16.7 mmol) and DIPEA (7.8 mL, 45 mmol) were sequentially added. The reaction mixture was stirred at RT overnight, cooled, then filtered. The white solid was triturated with EtOAc, filtered and dried to give **39b** (450 mg, 8%).

**N-[7-Methoxy-8-[3-(morpholin-4-yl)propoxy]-2,3-dihydroimidazo[1,2-c]quinazolin-5-yl]isonicotinamide (39c):** To a vigorously stirred solution of amine **36** (50% purity; 100 mg, 139  $\mu$ mol) in DMF (2.0 mL) was added isonicotinic acid (25.7 mg, 209  $\mu$ mol), followed by DIPEA (97  $\mu$ L, 560  $\mu$ mol) and PyBOP (109 mg, 209  $\mu$ mol). After a few seconds a clear brown solution was obtained, then a thick slurry immediately formed. Stirring was continued overnight. The slurry was filtered and the solid was washed with EtOAc to give **39c** as a white solid (30 mg, 46%); MS (ESI+)  $m/z$  (%): 465 (100)  $[M+H]^+$ ; HRMS-ESI  $m/z$   $[M+H]^+$  calcd for  $C_{24}H_{29}N_6O_4$ : 465.2250, found: 465.2249.

**2-Amino-N-[7-methoxy-8-[3-(morpholin-4-yl)propoxy]-2,3-dihydroimidazo[1,2-c]quinazolin-5-yl]isonicotinamide (39d):** Amine **36** (100 mg, 0.28 mmol) was dissolved in DMF (3 mL), and 2-aminoisonicotinic acid (38 mg, 0.28 mmol) was added. PyBOP (217 mg, 0.42 mmol) and DIPEA (0.15 mL, 0.83 mmol) were sequentially added, and the mixture was stirred at RT overnight and then concentrated under reduced pressure. Purification by HPLC gave **39d** (50 mg, 37%);  $^1H$  NMR ( $[D_6]DMSO$ ):  $\delta$  = 2.25 (m, 2H), 3.13 (m, 2H), 3.31 (brt, 2H), 3.50 (d, 2H), 3.66 (t, 2H), 3.99 (brs, 2H), 4.01 (s, 3H), 4.27 (dd, 2H), 4.35 (brt, 2H), 4.50 (dd, 2H), 7.38 (dd, 1H), 7.50 (d, 1H), 7.75 (s, 1H), 8.06 (d, 1H), 8.08 (s, 1H), 8.42 (brs, 1H), 10.15 (brs, 1H), 13.25 ppm (brs, 1H); MS (ESI+)  $m/z$ : 480.3  $[M+H]^+$ .

**6-Amino-N-[7-methoxy-8-[3-(morpholin-4-yl)propoxy]-2,3-dihydroimidazo[1,2-c]quinazolin-5-yl]nicotinamide (39e):** To amine **36** (150 mg, 417  $\mu$ mol) and 6-aminonicotinic acid (69.2 mg, 501  $\mu$ mol) dissolved in anhydrous DMF (10 mL) was added DIPEA (218  $\mu$ L, 1.25 mmol), then PyBOP (261 mg, 501  $\mu$ mol), and the reaction mixture was stirred at RT for 18 h. Amide **39e** was collected

by filtration, washed with water (20 mL) and oven-dried (112 mg, 56%):  $^1\text{H}$  NMR ( $[\text{D}_6]\text{DMSO}$ ):  $\delta$  = 1.88–2.02 (m, 2H), 2.32–2.42 (m, 4H), 2.43–2.47 (m, 2H), 3.53–3.63 (m, 4H), 3.90 (s, 3H), 4.03 (dd, 4H), 4.15 (t, 2H), 6.43 (d, 1H), 6.63 (s, 2H), 7.01 (d, 1H), 7.58 (d, 1H), 8.04 (dd, 1H), 8.78 (d, 1H), 12.88 ppm (s, 1H); MS (ESI $^-$ )  $m/z$ : 478  $[\text{M}-\text{H}]^+$ .

**6-(Dimethylamino)-*N*-[7-methoxy-8-[3-(morpholin-4-yl)propoxy]-2,3-dihydroimidazo[1,2-*c*]quinazolin-5-yl]nicotinamide (39f):** Amine **36** (50% purity; 150 mg, 209  $\mu\text{mol}$ ) and 6-(dimethylamino)-nicotinic acid (69.4 mg, 417  $\mu\text{mol}$ ) were suspended in DMF (2.0 mL) and DIPEA (110  $\mu\text{L}$ , 630  $\mu\text{mol}$ ). Then, solid PyBOP (217 mg, 417  $\mu\text{mol}$ ) was added all at once. The mixture was stirred at RT for 3 d. The precipitate was collected by filtration, washed with EtOAc and dried in a vacuum oven at 50 °C for 1 h to give **39f** (53.7 mg, 51%).

***N*-[7-Methoxy-8-[3-(morpholin-4-yl)propoxy]-2,3-dihydroimidazo[1,2-*c*]quinazolin-5-yl]pyrazine-2-carboxamide (39g):** Amine **36** (50% purity; 150 mg, 209  $\mu\text{mol}$ ) and pyrazine-2-carboxylic acid (51.8 mg, 417  $\mu\text{mol}$ ) were suspended in DMF (1.0 mL) and DIPEA (110  $\mu\text{L}$ , 630  $\mu\text{mol}$ ). Solid PyBOP (217 mg, 417  $\mu\text{mol}$ ) was added all at once. The mixture was stirred at RT for 7 d. The white solids were collected by filtration, washed copiously with EtOAc and dried in a vacuum oven at 45 °C overnight to give **39g** (59 mg, 61%).

***N*-[7-Methoxy-8-[3-(morpholin-4-yl)propoxy]-2,3-dihydroimidazo[1,2-*c*]quinazolin-5-yl]pyrimidine-5-carboxamide (39h):** Amine **36** (80% purity; 100 mg, 0.22 mmol) was dissolved in DMF (5 mL), and pyrimidine-5-carboxylic acid (41 mg, 0.33 mmol) was added. PyBOP (173 mg, 0.33 mmol) and DIPEA (0.16 mL, 0.89 mmol) were sequentially added, and the mixture was stirred at RT overnight. EtOAc was added, and the precipitate was isolated by vacuum filtration to give **39h** (12 mg, 11%):  $^1\text{H}$  NMR ( $[\text{D}_6]\text{DMSO} + 2$  drops  $[\text{D}]\text{TFA}$ ):  $\delta$  = 2.27 (m, 2H), 3.16 (m, 2H), 3.33 (m, 2H), 3.52 (m, 2H), 3.67 (brt, 2H), 4.00 (m, 2H), 4.02 (s, 3H), 4.26 (m, 2H), 4.35 (brt, 2H), 4.59 (m, 2H), 7.47 (d, 1H), 8.05 (d, 1H), 9.39 (s, 1H), 9.48 (s, 2H); MS (ESI $^+$ )  $m/z$ : 466  $[\text{M}+\text{H}]^+$ ; HRMS-ESI  $m/z$   $[\text{M}+\text{H}]^+$  calcd for  $\text{C}_{23}\text{H}_{28}\text{N}_7\text{O}_4$ : 466.2203, found: 466.2203.

**2-Aminopyrimidine-5-carboxylic acid (39i):** Sodium (1Z)-2-(dimethoxymethyl)-3-methoxy-3-oxoprop-1-en-1-olate (1.37 g, 6.9 mmol), prepared as reported,<sup>[37]</sup> was dissolved in DMF (12 mL), and guanidine hydrochloride (640 mg, 6.7 mmol) was added. The mixture was stirred at 100 °C for 1 h, then cooled to RT and diluted with water. Methyl 2-aminopyrimidine-5-carboxylate precipitated as a light yellow solid, which was isolated by vacuum filtration (510 mg, 50%):  $^1\text{H}$  NMR ( $[\text{D}_6]\text{DMSO}$ ):  $\delta$  = 3.79 (s, 3H), 7.56 (brs, 2H), 8.67 (s, 2H). Methyl 2-aminopyrimidine-5-carboxylate (300 mg, 2.0 mmol) was dissolved in MeOH (5 mL) containing a few drops of water. Lithium hydroxide (122 mg, 5.1 mmol) was added, and the reaction mixture was stirred at 60 °C overnight. The mixture was concentrated under reduced pressure, then diluted with water, and the solution was adjusted to pH 4 with HCl (1 N). 2-Aminopyrimidine-5-carboxylic acid (**39i**) precipitated as a white solid, which was isolated by vacuum filtration (244 mg, 90%):  $^1\text{H}$  NMR ( $[\text{D}_6]\text{DMSO}$ ):  $\delta$  = 7.44 (brs, 2H), 8.63 (s, 2H), 12.73 (brs, 1H).

**2-Amino-*N*-[7-methoxy-8-[3-(morpholin-4-yl)propoxy]-2,3-dihydroimidazo[1,2-*c*]quinazolin-5-yl]pyrimidine-5-carboxamide (BAY 80-6946, 39i):** Amine **36** (80% purity; 100 mg, 0.22 mmol) was dissolved in DMF (5 mL), and acid **39i** (46 mg, 0.33 mmol) was added. PyBOP (173 mg, 0.33 mmol) and DIPEA (0.16 mL, 0.89 mmol) were sequentially added, and the mixture was stirred at RT overnight. EtOAc was added, and the solids were isolated by

vacuum filtration to give **39i** (42.7 mg, 40%):  $^1\text{H}$  NMR ( $[\text{D}_6]\text{DMSO} + 2$  drops  $[\text{D}]\text{TFA}$ ):  $\delta$  = 2.25 (m, 2H), 3.18 (m, 2H), 3.31 (m, 2H), 3.52 (m, 2H), 3.65 (brt, 2H), 4.00 (s, 3H), 4.04 (m, 2H), 4.23 (m, 2H), 4.34 (brt, 2H), 4.54 (m, 2H), 7.43 (d, 1H), 8.04 (d, 1H), 9.01 (s, 2H);  $^1\text{H}$  NMR of the bis-HCl salt (500 MHz,  $[\text{D}_6]\text{DMSO}$ ):  $\delta$  = 2.30–2.37 (m, 2H), 3.11 (brs, 2H), 3.25–3.31 (m, 2H), 3.48 (d,  $J$  = 12.1 Hz, 2H), 3.83–3.90 (m, 2H), 3.95–4.00 (m, 2H), 4.01 (s, 3H), 4.17–4.22 (m, 2H), 4.37 (t,  $J$  = 6.0 Hz, 2H), 4.47 (t,  $J$  = 9.7 Hz, 2H), 7.40 (d,  $J$  = 9.2 Hz, 1H), 7.54 (s, 2H), 8.32 (d,  $J$  = 9.2 Hz, 1H), 8.96 (s, 2H), 11.46 (brs, 1H), 12.92 (brs, 1H), 13.41 (brs, 1H);  $^{13}\text{C}$  NMR (125 MHz,  $[\text{D}_6]\text{DMSO}$ ):  $\delta$  = 23.09, 45.22, 46.00, 51.21, 53.38, 61.54, 63.40, 67.09, 101.18, 112.55, 118.51, 123.96, 132.88, 134.35, 148.96, 157.25, 160.56, 164.96, 176.02 ppm; MS (ESI $^+$ )  $m/z$ : 481  $[\text{M}+\text{H}]^+$ .

**2-Amino-4-methylpyrimidine-5-carboxylic acid (39j):** To a solution of ethyl 2-amino-4-methylpyrimidine-5-carboxylate (1.00 g, 5.52 mmol) in MeOH (27 mL) and THF (41 mL) was added NaOH (2 N, 14 mL), and the reaction mixture was stirred at RT overnight. Then, the mixture was neutralized with HCl (1 N, 20 mL), concentrated to ~30 mL under reduced pressure and filtered to give **39j** (0.6 g, 71%): MS (ESI $^+$ )  $m/z$ : 154  $[\text{M}+\text{H}]^+$ .

**2-Amino-*N*-[7-methoxy-8-[3-(morpholin-4-yl)propoxy]-2,3-dihydroimidazo[1,2-*c*]quinazolin-5-yl]-4-methylpyrimidine-5-carboxamide (39j):** To a solution of amine **36** (100 mg, 278  $\mu\text{mol}$ ) and acid **39j** (42.6 mg, 278  $\mu\text{mol}$ ) in anhydrous DMF (3.0 mL) was added DIPEA (150  $\mu\text{L}$ , 830  $\mu\text{mol}$ ) and PyBOP (217 mg, 417  $\mu\text{mol}$ ). The mixture was stirred at RT overnight. The precipitate was collected by filtration and washed with MeOH to give **39j** (93 mg, 68%): MS (ESI $^+$ )  $m/z$ : 495  $[\text{M}+\text{H}]^+$ .

**X-ray structure of copanlisib (BAY 80-6946, 39i) in complex with PI3K $\gamma$ :** Protein was expressed in insect cells and purified using Ni affinity chromatography, ion-exchange chromatography (Resource Q) and size exclusion chromatography (Superdex 200 26/60). The protein was concentrated to 5 mg mL $^{-1}$  in Tris (20 mM, pH 7.2),  $(\text{NH}_4)_2\text{SO}_4$  (0.5 mM), ethylene glycol (1%), CHAPS (0.02%) and DTT (5 mM). Prior to crystallization, copanlisib (2 mM) was added to the protein. Crystals were obtained using the sitting drop method by mixing an equal volume of protein and reservoir solution (1  $\mu\text{L} + 1 \mu\text{L}$ ). Crystals were obtained using PEG 4000 (19%),  $(\text{NH}_4)_2\text{SO}_4$  (0.15 M) and Tris (0.1 M, pH 7.5). Data were collected at the synchrotron facility at the SLS in Villigen, Switzerland. The structure was solved using 2CHX as search model. The structure was refined using REFMAC within the CCP4 suite. The crystallographic data for the structure have been deposited with the RCSB Protein Data Bank (PDB) with access code 5G2N.

## Acknowledgements

We thank Dr. S. Gruendemann and Dr. G. Depke for their support regarding analytical data, and C. Moldenhauer, S. Korthals, and Dr. K. Greenfield for valuable technical support with the manuscript. We thank Proteros Biostructures for the X-ray structure determination of copanlisib. We also thank Dr. F. von Nussbaum for very stimulating discussions and Prof. H. Wild for his support.

**Keywords:** phosphoinositide 3-kinase • copanlisib • lipid kinases • PI3K inhibitors • X-ray crystallography

[1] L. C. Cantley, *Science* **2002**, 296, 1655–1657.

[2] B. Vanhaesebroeck, M. A. Whitehead, R. Pineiro, *J. Mol. Med.* **2016**, 94, 5–11.



- [3] T. M. Bauer, M. R. Patel, J. R. Infante, *Pharmacol. Ther.* **2015**, *146*, 53–60.
- [4] B. Vanhaesebroeck, M. D. Waterfield, *Exp. Cell Res.* **1999**, *253*, 239–254.
- [5] L. M. Thorpe, H. Yuzugullu, J. J. Zhao, *Nat. Rev. Cancer* **2015**, *15*, 7–24.
- [6] P. K. Vogt, J. R. Hart, M. Gymnopoulos, H. Jiang, S. Kang, A. G. Bader, Z. Li, A. Denley, *Curr. Top. Microbiol. Immunol.* **2010**, *347*, 79–104.
- [7] Y. Samuels, Z. Wang, A. Bardelli, N. Silliman, J. Ptak, S. Szabo, H. Yan, A. Gazdar, S. M. Powell, G. J. Riggins, J. K. V. Willson, S. Markowitz, K. W. Kinzler, B. Vogelstein, V. E. Velculescu, *Science* **2004**, *304*, 554.
- [8] G. Ligresti, L. Militello, L. S. Steelman, A. Cavallaro, F. Basile, F. Nicoletti, F. Stivala, J. A. McCubrey, M. Libra, *Cell Cycle* **2009**, *8*, 1352–1358.
- [9] K.-K. Wong, J. A. Engelman, L. C. Cantley, *Curr. Opin. Genet. Dev.* **2010**, *20*, 87–90.
- [10] M.-M. Georgescu, *Genes Cancer* **2010**, *1*, 1170–1177.
- [11] R. Parsons, *Semin. Cell Dev. Biol.* **2004**, *15*, 171–176.
- [12] M. S. Song, L. Salmena, P. P. Pandolfi, *Nat. Rev. Mol. Cell Biol.* **2012**, *13*, 283–296.
- [13] S. Wee, D. Wiederschain, S.-M. Maira, A. Loo, C. Miller, R. de Beaumont, F. Stegmeier, Y.-M. Yao, C. Lengauer, *Proc. Natl. Acad. Sci. USA* **2008**, *105*, 13057–13062.
- [14] K. A. Edgar, J. J. Wallin, M. Berry, L. B. Lee, W. W. Prior, D. Sampath, L. S. Friedman, M. Belvin, *Cancer Res.* **2010**, *70*, 1164–1172.
- [15] H. A. Dbouk, J. M. Backer, *Oncotarget* **2010**, *1*, 729–733.
- [16] S. W. Brady, J. Zhang, D. Seok, H. Wang, D. Yu, *Mol. Cancer Ther.* **2014**, *13*, 60–70.
- [17] M. Mao, F. Tian, J. M. Mariadason, C. C. Tsao, R. Lemos, Jr., F. Dayyani, Y. N. V. Gopal, Z.-Q. Jiang, I. I. Wistuba, X. M. Tang, W. G. Bornman, G. Bollag, G. B. Mills, G. Powis, J. Desai, G. E. Gallick, M. A. Davies, S. Kopetz, *Clin. Cancer Res.* **2013**, *19*, 657–667.
- [18] L. Y. Huw, C. O'Brien, A. Pandita, S. Mohan, J. M. Spoerke, S. Lu, Y. Wang, G. M. Hampton, T. R. Wilson, M. R. Lackner, *Oncogenesis* **2013**, *2*, e83.
- [19] X. Xie, B. Tang, J. Zhou, Q. Gao, P. Zhang, *Oncol. Rep.* **2013**, *30*, 773–782.
- [20] A. K. Gupta, G. J. Cerniglia, R. Mick, M. S. Ahmed, V. J. Bakanauskas, R. J. Muschel, W. G. McKenna, *Int. J. Radiat. Oncol. Biol. Phys.* **2003**, *56*, 846–853.
- [21] G. Konstantinidou, E. A. Bey, A. Rabellino, K. Schuster, M. S. Maira, A. F. Gazdar, A. Amici, D. A. Boothman, P. P. Scaglioni, *Cancer Res.* **2009**, *69*, 7644–7652.
- [22] X. Zhang, X.-r. Li, J. Zhang, *Curr. Cancer Drug Targets* **2013**, *13*, 175–187.
- [23] C. Massacesi, E. di Tomaso, N. Fretault, S. Hirawat, *Ann. N. Y. Acad. Sci.* **2013**, *1280*, 19–23.
- [24] W. A. Denny, *Expert Opin. Ther. Pat.* **2013**, *23*, 789–799.
- [25] T. A. Yap, L. Bjerke, P. A. Clarke, P. Workman, *Curr. Opin. Pharmacol.* **2015**, *23*, 98–107.
- [26] A. Markham, *Drugs* **2014**, *74*, 1701–1707.
- [27] S. Chandarlapaty, A. Sawai, M. Scaltriti, V. Rodrik-Outmezguine, O. Grbovic-Huezo, V. Serra, P. K. Majumder, J. Baselga, N. Rosen, *Cancer Cell* **2011**, *19*, 58–71.
- [28] A. Carracedo, P. P. Pandolfi, *Oncogene* **2008**, *27*, 5527–5541.
- [29] E. Halilovic, Q.-B. She, Q. Ye, R. Pagliarini, W. R. Sellers, D. B. Solit, N. Rosen, *Cancer Res.* **2010**, *70*, 6804–6814.
- [30] E. H. Walker, O. Perisic, C. Ried, L. Stephens, R. L. Williams, *Nature* **1999**, *402*, 313–320.
- [31] E. H. Walker, M. E. Pacold, O. Perisic, L. Stephens, P. T. Hawkins, M. P. Wymann, R. L. Williams, *Mol. Cell* **2000**, *6*, 909–919.
- [32] Z. A. Knight, B. Gonzalez, M. E. Feldman, E. R. Zunder, D. D. Goldenberg, O. Williams, R. Loewith, D. Stokoe, A. Balla, B. Toth, T. Balla, W. A. Weiss, R. L. Williams, K. M. Shokat, *Cell* **2006**, *125*, 733–747.
- [33] M. Andrs, J. Korabecny, D. Jun, Z. Hodny, J. Bartek, K. Kuca, *J. Med. Chem.* **2015**, *58*, 41–71.
- [34] A. Berndt, S. Miller, O. Williams, D. D. Le, B. T. Houseman, J. I. Pacold, F. Gorrec, W.-C. Hon, Y. Liu, C. Rommel, P. Gaillard, T. Rueckle, M. K. Schwarz, K. M. Shokat, J. P. Shaw, R. L. Williams, *Nat. Chem. Biol.* **2010**, *6*, 117–124.
- [35] J. R. Somoza, D. Koditek, A. G. Villaseñor, N. Novikov, M. H. Wong, A. Licican, W. Xing, L. Lagpacan, R. Wang, B. E. Schultz, G. A. Papalia, D. Samuel, L. Lad, M. E. McGrath, *J. Biol. Chem.* **2015**, *290*, 8439–8446.
- [36] T. D. Cushing, X. Hao, Y. Shin, K. Andrews, M. Brown, M. Cardozo, Y. Chen, J. Duquette, B. Fisher, F. Gonzalez-Lopez de Turiso, X. He, K. R. Henne, Y.-L. Hu, R. Hungate, M. G. Johnson, R. C. Kelly, B. Lucas, J. D. McCarter, L. R. McGee, J. C. Medina, T. San Miguel, D. Mohn, V. Pattaropong, L. H. Pettus, A. Reichelt, R. M. Rzasa, J. Seganish, A. S. Tasker, R. C. Wahl, S. Wannberg, D. A. Whittington, J. Whoriskey, G. Yu, L. Zalameda, D. Zhang, D. P. Metz, *J. Med. Chem.* **2015**, *58*, 480–511.
- [37] M. Shimada, T. Murata, K. Fuchikami, H. Tsujishita, N. Omori, I. Kato, M. Miura, K. Urbahns, F. Gantner, K. Bacon (Bayer Pharmaceuticals Corp.), WO 2004029055 (20030918), **2004**.
- [38] S. F. MacDonald, *J. Chem. Soc.* **1948**, 376–378.
- [39] K. H. Slotta, F. Lauersen, *J. Prakt. Chem.* **1934**, *139*, 220–228.
- [40] W. H. Moos, R. D. Gless, H. Rapoport, *J. Org. Chem.* **1981**, *46*, 5064–5074.
- [41] R. Ahmad, J. M. Saa, M. P. Cava, *J. Org. Chem.* **1977**, *42*, 1228–1230.
- [42] M. Hentemann, J. Wood, W. J. Scott, M. Michels, A.-M. Campbell, A.-M. Bullion, R. B. Rowley, A. Redman (Bayer Schering Pharma AG), WO 2008070150 (20071205), **2008**.
- [43] N. Liu, R. B. Rowley, C. O. Bull, C. Schneider, A. Haegbarth, C. A. Schatz, P. R. Fracasso, D. P. Wilkie, M. Hentemann, S. M. Wilhelm, W. J. Scott, D. Mumberg, K. Ziegelbauer, *Mol. Cancer Ther.* **2013**, *12*, 2319–2330.

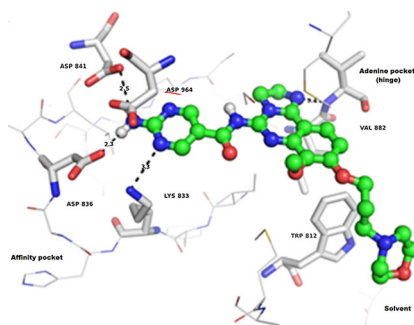
Received: March 11, 2016

Revised: May 12, 2016

Published online on ■■■ ■■, 0000

## FULL PAPERS

**The phosphoinositide 3-kinase (PI3K)** pathway is aberrantly activated in many tumors. The presence of various PI3K isoforms and their differential roles in cancers makes them ideal candidates for targeted inhibition. A PI3K $\gamma$  screening hit led to the discovery of the novel 2,3-dihydroimidazo[1,2-*c*]quinazoline class of PI3K inhibitors. Herein we describe initial structure–activity relationship findings for this class and the optimization that led to the identification of copanlisib (BAY 80-6946) as a clinical candidate.



W. J. Scott,\* M. F. Hentemann, R. B. Rowley, C. O. Bull, S. Jenkins, A. M. Bullion, J. Johnson, A. Redman, A. H. Robbins, W. Esler, R. P. Fracasso, T. Garrison, M. Hamilton, M. Michels, J. E. Wood, D. P. Wilkie, H. Xiao, J. Levy, E. Stasik, N. Liu, M. Schaefer, M. Brands, J. Lefranc\*



**Discovery and SAR of Novel 2,3-Dihydroimidazo[1,2-*c*]quinazoline PI3K Inhibitors: Identification of Copanlisib (BAY 80-6946)**

